Inorganic Chemistry

Article

pubs.acs.org/IC

Are Very Small Emission Quantum Yields Characteristic of Pure Metal-to-Ligand Charge-Transfer Excited States of Ruthenium(II)-(Acceptor Ligand) Chromophores?

Chia Nung Tsai,[†] Shivnath Mazumder,[‡] Xiu Zhu Zhang,[†] H. Bernhard Schlegel,*[,‡] Yuan Jang Chen,*[,†,‡] and John F. Endicott*[,‡]

[†]Department of Chemistry, Fu-Jen Catholic University, New Taipei City 24205, Taiwan, Republic of China

[‡]Department of Chemistry, Wayne State University, Detroit, Michigan 48202, United States

Supporting Information

ABSTRACT: Metal to ligand charge-transfer (MLCT) excited state emission quantum yields, ϕ_{em}, are reported in 77 K glasses for a series of pentaammine and tetraammine ruthenium(II) complexes with monodentate aromatic acceptor ligands (Ru-MDA) such as pyridine and pyrazine. These quantum yields are only about 0.2−1% of those found for their Ru-bpy (bpy = 2,2′-bipyridine) analogs in similar excited state energy ranges ($h\nu_{em}$). The excited state energy dependencies of the emission intensity are characterized by mean radiative decay rate constants, k_{RAD}, resolved from $\phi_{em}/\tau_{obs} = k_{RAD}$ (τ_{obs} = the observed emission decay lifetime; $\tau_{obs}^{-1} = k_{RAD} + k_{NRD}$; k_{NRD} = nonradiative decay rate constant). Except for the Ru-pz chromophores in alcohol glasses, the values of k_{NRD} for the Ru-MDA chromophores are slightly smaller, and their dependences on excited state energies are very similar to those of related Ru-bpy chromophores. In principle, one expects k_{RAD} to be proportional to the product of $(h\nu_{em})^3$ and the square of the transition dipole moment ($M_{e,g}$).[2] However, from experimental studies of Ru-bpy chromophores, an additional $h\nu_{em}$ dependence has been found that originates in an intensity stealing from a higher energy excited state with a much larger value of $M_{e,g}$. This additional $h\nu_{em}$ dependence is not present in the k_{RAD} energy dependence for Ru-MDA chromophores in the same energy regime. Intensity stealing in the phosphorescence of these complexes is necessary since the triplet-to-singlet transition is only allowed through spin−orbit coupling and since the density functional theory modeling implicates configurational mixing between states in the triplet spin manifold; this is treated by setting $M_{e,g}$ equal to the product of a mixing coefficient and the difference between the molecular dipole moments of the states involved, which implicates an experimental first order dependence of k_{RAD} on $h\nu_{em}$. The failure to observe intensity stealing for the Ru-MDA complexes suggests that their weak emissions are more typical of "pure" (or unmixed) ^{3}MLCT excited states.

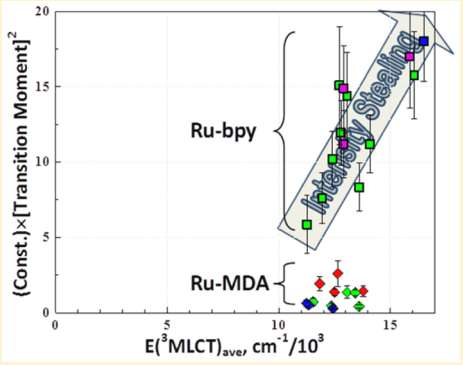

INTRODUCTION

The lowest energy triplet metal-to-ligand-charge-transfer (^{3}MLCT) excited states of ruthenium(II) complexes with aromatic ligand acceptors (Ru-A) have been of interest for some time because these complexes often have appreciable visible region absorptivity and their excited states can function as highly reactive electron transfer or substitutional reagents, which could lead to applications such as sensitizers for solar cells, photodiodes, photocatalysts, phototherapy, etc.[1−14] Despite this interest, there have been few studies that systematically vary the ^{3}MLCT energies of single Ru-A chromophores in order to characterize the excited state nuclear distortions and electronic configurations that are generally as relevant to their optimization for particular applications as are the excited state energies.[15] Such studies necessitate the examination of series of complexes in which key properties are varied systematically, but because the excited state lifetimes are short (in the sub-ns to sub-ms range) even in low temperature glasses, the most convenient experimental probes of ^{3}MLCT excited states are based on their luminescence properties combined with theoretical modeling of the excited states.[16−19] The excited state electronic configurations rarely have known ground state analogs, and there are a very large number of electronic excited states of transition metal complexes that are near in energy for which the presumed excited state electronic configurations can mix (see Yersin et al.).[14] As a consequence, the electronic and molecular structural models of the reactive excited states that are often based on extrapolations from known ground state species are likely to be misleading, and configurational mixing among the presumed electronic excited states can alter their energies, electronic structures, nuclear distortions (and related emission band-shapes),[16,20,21] lifetimes (or emission decay rate constants = k_{obs}),[17,22,23] transition moments (through "intensity stealing"),[24] and other donor/acceptor properties.[16,17,19,22,24,25]

Received: February 13, 2016
Published: July 20, 2016

DOI: 10.1021/acs.inorgchem.6b00374
Inorg. Chem. 2016, 55, 7341−7355

The Ru-A complexes are among the most useful for systematic studies of transition metal excited state properties since substitution inert ground state complexes with a wide variety of ancillary and acceptor ligands can be synthesized, and at low temperatures their lowest energy MLCT excited states generally have sufficiently small values of k_{obs} that their emissions can be conveniently observed and the electronic and the nuclear structures of their lowest energy ^{3}MLCT excited states can be computationally modeled using the Franck−Condon approximation as implemented in density functional theory (DFT) with only the packaged atomic parameters.[7,16−19,24,26−47] Our recent work has indicated that systematic variations in emission bandshapes and intrinsic intensities (manifested in quantum yields and radiative rate constants; see below) can be useful probes of mixing between ^{3}MLCT and other excited states.[17,24,45] Thus, the vibronic sidebands in the observed emission spectra, and by inference the excited state distortions, of ruthenium(II)-(2,2′-bipyridine)-(Ru-bpy) chromophores increase in significance as the energy of the emitting ^{3}MLCT excited state increases.[21,48,49] This would not be expected for a simple donor−acceptor system,[16,24] and our DFT modeling of the triplet manifold has largely reproduced the excited state distortions inferred from resonance-Raman (rR) spectra as well as the variations in vibronic sidebands observed in the emission spectra of Ru-A chromophores (where the electron acceptor A = bpy, pyrazine (pz), quinoline, etc.).[7,16−19,24] Furthermore, the increasing significance of vibronic sidebands with increasing emission energy found for the Ru-bpy chromophores is correlated with the increases in intrinsic emission intensities as manifested in increases in the radiative rate constant (k_{RAD}; see eqs 1−3), and our DFT modeling indicated that the detailed triplet-manifold mixing is between the pπ(bpy$^{\bullet-}$) orbitals of the reduced acceptor with the hole in a metal centered singly occupied molecular orbital (dπ−SOMO) in the ^{3}MLCT excited state, corresponding to ^{3}MLCT/$^3\pi\pi^*$ excited state/excited state mixing.[16,17,24]

In the simplest cases, k_{RAD} is obtained from the experimentally determined emission quantum yield, ϕ_{em}, and the excited state decay rate constant, k_{obs}, by means of eqs 1 and 2

$$\phi_{em} = \frac{k_{RAD}}{k_{RAD} + k_{NRD} + k_{other}} = \frac{k_{RAD}}{k_{obs}} \quad (1)$$

$$k_{obs} = k_{RAD} + k_{NRD} + k_{other} \quad (2)$$

In eq 2, k_{NRD} is the rate constant for nonradiative decay of the emitting excited state directly to the ground electronic state, while other excited state quenching processes, such as internal conversion (IC) and intersystem crossing (ISC) to lower energy excited states or intermolecular electron or energy transfer reactions, are included in k_{other}. When $k_{other} \ll (k_{RAD} + k_{NRD})$, eqs 1 and 2 can be used to resolve k_{RAD} and k_{NRD}. Values of k_{NRD} are expected to be functions only of the energy difference between the emitting state and the ground state and the intramolecular distortion coordinates.[50−52] In this report, we find that values of k_{NRD} are generally slightly smaller but follow very similar patterns for the Ru-MDA (MDA a monodentate aromatic acceptor ligand) and Ru-bpy chromophores.

The radiative rate constant is an experimental measure of the emission intensity in the limit of no competing relaxation processes. It is an average of all spectral contributions and a function of the excited state energy and the transition dipole moment, $M_{e,g}$[52−56]

$$k_{RAD} = C_r(\nu_{e,g})^3\eta^3(M_{e,g})^2 \quad (3)$$

where $\nu_{e,g}$ is the vertical energy difference between the excited and ground states, η is the refractive index of the matrix, $C_r = (16\pi^3)/(3\varepsilon_o c^3 h)$, and ε_o is the vacuum permittivity.

Issues pertinent to electronic coupling matrix elements, $H_{e,g}$, have been discussed extensively in the literature[22,23,25,56−65] and are the basis for the treatment in this report. The transition moment can be represented as a function of $H_{e,g}$ and the diabatic energy difference between the states that are mixed, $\Delta E^{dia}_{e,g} = |E^{dia}_e - E^{dia}_g|$ (see Figure 1).[22,23,56,58,64,66] The general

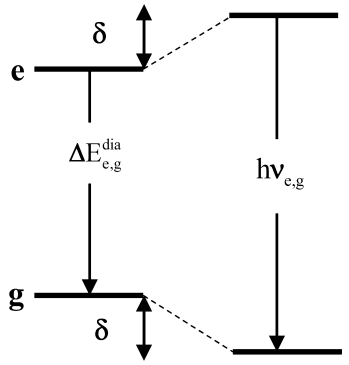

Figure 1. A simple diagrammatic illustration of the mixing of two states.

relationship between $M_{e,g}$ and $H_{e,g}$ in a two state limit varies with the magnitude of $\Delta E^{dia}_{e,g}$. When $\Delta E^{dia}_{e,g} \gg H_{e,g}$, $M_{e,g}$ can be represented as

$$\overrightarrow{M_{e,g}} = \alpha_{e,g}\overrightarrow{\Delta\mu_{e,g}} \quad (4)$$

where the mixing coefficient is $\alpha_{e,g} = H_{e,g}/\Delta E^{dia}_{e,g}$, $H_{e,g}$ is a function of the electronic configurations of states e and g, and $\Delta\mu_{e,g}$ is the difference between excited and ground state molecular dipole moments.[58] The mixing mediated by $H_{e,g}$ results in adiabatic states which differ more in energy: $\Delta E^{ad}_{e,g} > \Delta E^{dia}_{e,g}$ as illustrated in Figure 1; $\Delta E^{ad}_{e,g} = h\nu_{e,g}$ is the vertical energy difference between the mixed (adiabatic) states at the point of transition. Cave and Newton have developed a more general form of eq 4 to deal with situations where $H_{e,g}$ is significant compared to $\Delta E^{dia}_{e,g}$.[61]

In electron rich donor/acceptor systems, such as those in this report, there is a potential for mixing between the different excited states, and such excited state/excited state mixing can alter the energy dependence observed for k_{RAD}. In such cases, one must consider the interactions between three or more electronic states even for spin allowed transitions. There are two limiting cases considered in the literature: (a) When a donor/acceptor (D/A) system has a very strong spin allowed transition localized on the D or A moiety (e.g., A → A*), it can mix with a weak charge transfer transition, (D,A) → (D$^+$,A$^-$), thereby enhancing the intensity observed for the donor−acceptor charge transfer (DACT) transition. This kind of mixing has been discussed by Mulliken and Person,[58] by Bixon et al.,[66] and by Gould and co-workers[25] for fluorescent systems. (b) The excited state-to-ground state transitions in phosphorescent systems require some mixing between singlet and triplet

DOI: 10.1021/acs.inorgchem.6b00374
Inorg. Chem. 2016, 55, 7341−7355

excited states through a spin−orbit coupling (SOC) perturbation in order for an emission to be observed.

For a strongly allowed transition to a higher energy acceptor ligand localized transition (LL) whose ($\alpha_{e,LL}$) is sufficiently large that it can significantly alter the values of $M_{e,g}$, the transition moment for a spin allowed transition becomes[58]

$$\vec{M}_{eg} \approx (\overrightarrow{M_{e,g(0)}} + \alpha_{e,LL}\overrightarrow{M_{LL,g(0)}})N \quad (5)$$

where N is the normalizing constant and $\overrightarrow{M_{x,g(0)}}$ (x = e or LL) designates the transition moment with no mixing of the excited states. The vector notation is used because the transition dipole moments may not be collinear. Combining eqs 3 and 5 (and assuming that $\overrightarrow{M_{e,g(0)}}$ and $\overrightarrow{M_{LL,g(0)}}$ are approximately orthogonal (approximately axial MLCT and $\pi\pi^*$ orthogonal to bpy ring in Ru-bpy; the general case is discussed by Bixon et al.[66])) leads to a more general expression for k_{RAD} for spin-allowed transitions:

$$k_{RAD} \approx C_r(\nu_{e,g})^3\eta^3(M^2_{e,g(0)} + \alpha^2_{e,LL}M^2_{LL,g(0)}) \quad (6)$$

The two transition moment components in eq 6 correspond respectively to (a) the "pure" transition between the states e and g ($M^2_{e,g(0)}$) and (b) the result of configurational mixing with the ligand centered excited state ($\alpha^2_{e,LL}M^2_{LL,g(0)}$); $M_{LL,g(0)}$ is the transition dipole moment for the LL → g transition in the absence of excited state mixing. The second transition moment component of eq 6 implies increases in emission intensity as the energy difference $\Delta E^{dia}_{e,LL}$ decreases; since $\Delta E_{e,LL}$ will decrease as $\nu_{e,g}$ increases, this effect will appear as an "additional" energy dependence of the emission intensity. Our previous work has found that the observed energy dependent contributions of the vibronic sidebands of Ru-bpy complexes[20,21] are very well reproduced by DFT modeling of the configurational mixing of ^{3}MLCT/$^3\pi\pi^*$ excited states in these complexes and that this mixing correlates with an "extra" energy dependence of k_{RAD}, qualitatively consistent with eq 6.[16,24]

Since the transitions considered here are ^{3}MLCT → S_0, they are only allowed by SOC between excited states.[22,23,64,67] This mixing can be described by an equation analogous to eq 5 which accounts for the spin (symmetric and antisymmetric representations for triplet and singlet, respectively in the C_2 or C_s point groups)[68] as well as the orbital symmetries which are appropriate for combination with the ^{3}MLCT electronic wave functions. However, when there is also configurational mixing within the triplet manifold, the net result is very complicated. Thus, a ^{1}MLCT excited state has often been proposed as the state mediating the SOC mixing.[22,23,64] The ^{1}MLCT → S_0 transition moment for such a state would be more or less parallel to the ^{3}MLCT → S_0 moment, and when either the ^{3}MLCT excited state is mixed with other states in the triplet manifold and/or the ^{1}MLCT excited state is mixed with other states in the singlet manifold, the resulting expression for k_{RAD} is far more complex than eq 6.

The very different excited state energy ($h\nu_{e,g}$) dependencies of the radiative rate constant (and thereby the emission intensity) for a two state system in eqs 3 and 6 correspond to limiting solutions of the secular equation for the energies: $h\nu_{e,g} = [(\Delta E^{dia}_{e,g})^2 + 4H^2_{e,g}]^{1/2}$. Thus, in a two state system, the experimental energy dependence of k_{RAD} is expected to vary smoothly between the two corresponding limits:

M1: $k_{RAD} \propto (h\nu_{e,g})$ when $\Delta E^{dia}_{e,g} \gg H_{e,g}$

M2: $k_{RAD} \propto (h\nu_{e,g})^3$ for the special case $H_{e,g} \gg \Delta E^{dia}_{e,g}$

When configurational mixing within a spin-manifold and/or SOC are important, the functional dependence of k_{RAD} on $h\nu_{e,g}$ involves at least a three state system with an experimental dependence of k_{RAD} on $h\nu_{e,g}$ that may be very different from the above:

M3: The functional dependence of k_{RAD} on $h\nu_{e,g}$ can change in the higher energy regions from the M1 behavior to a stronger $h\nu_{e,g}$ dependence, as has been observed for the Ru-bpy chromophores.[24]

Previous experimental studies of energy dependence of k_{RAD} have dealt with spin allowed emission (fluorescence) in spatially separated donor/acceptor systems.[25,57] However, the arguments are very general, and the condition for "isolation" of the electronic states is that $H_{e,g} < \Delta E^{dia}_{e,g}$, which can result from orthogonality constraints as well as spatial separation, and the spin forbidden (phosphorescence) emissions discussed here could lead to the category M1 energy dependence of k_{RAD}. Electroabsorption studies of the dominant absorptions in Ru-A complexes (at approximately 20 000−30 000 cm^{-1}) have generally found large values of $H_{g,e}$ ($\lesssim 10^4$ cm^{-1}),[69,70] but the lowest energy $S_0 \rightarrow S_1$ transitions in these complexes tend to have very small oscillator strengths and consequently very small values of $H_{g,e}$.[71,72] Even the ground state metal/bipyridine electronic mixing appears to be very weak in many transition metal complexes,[42,43] and we have found no evidence for such mixing in DFT-calculated HOMOs and LUMOs of Ru-A complexes.[19,71,72] In view of these considerations and the spin-forbiddeness of the phosphorescent emissions of the Ru-A complexes, the values of $H_{e,g}$ for their ^{3}MLCT → S_0 transitions are expected to be very small, and their k_{RAD} energy dependence is most likely to fall into category 1 or 3, above.

There has been little systematic investigation of the energy dependence of k_{RAD} for the phosphorescent emissions of transition metal complexes, and models assuming that k_{RAD} for them falls into category 2 with the $(\nu_{e,g})^3$ dependence appear to be deeply embedded in the literature for these systems. For example, this assumption combined with the approximation that $M_{e,g}$ is constant has been employed in approaches for fitting a single emission spectrum.[73−76] While this approximation may be useful in such applications, it is not useful in the comparison of a series of different complexes with the same chromophore. In the present study, we examine the energy dependence of k_{RAD} for the very weakly emitting[18] $[(L)_5Ru(MDA)]^{m+}$ complexes (MDA = a monodentate aromatic ligand; L = an ancillary ligand).

EXPERIMENTAL SECTION

Materials and Synthesis of Compounds. Pyrazine (pz), pyridine (py), 4-acetylpyridine (ac-py), 4-phenylpyridine (ph-py), 4,4′-bipyridine (4,4′-bpy), 2,2′-bipyridine (bpy), 2,2′-bipyridylammine (bpyam), ferrocene, and trifluoromethanesulfonic acid (HOTf) were purchased from Aldrich, and $[Ru(NH_3)_6]Cl_3$ and NH_4PF_6 were purchased from STREM Chemicals. These materials were used without further purification. The syntheses of $[Ru(NH_3)_5Cl]Cl_2$, $[Ru(NH_3)_5(H_2O)](PF_6)_2$, *cis*-$[Ru(NH_3)_4(Cl)_2]Cl$, *trans*-$[Ru(NH_3)_4(L)(H_2O)](PF_6)_2$,[77,78] L = 4-phenyl-pyridine (ph-py), NH_3, and 4-acetyl-pyridine (ac-py) have been reported previously. Literature syntheses were used for the following compounds: $[Ru(NH_3)_5(L)]^{2+}$ complexes with L = pyridine (py), ac-py, ph-py, 4,4′-bipyridine (4,4′-bpy), and pyrazine (pz)[79−82] and *cis*-/*trans*-$[Ru(NH_3)_4(L)_2](PF_6)_2$ with L = pz, py, ac-py, and ph-py.[71,83−86] Variations in previously reported syntheses were used for the following compounds: *trans*-$[Ru(NH_3)_4(py)(pz)](PF_6)_2$,[85] *mer*-$[Ru(NH_3)_3(bpy)(L)](PF_6)_2$ (L =

DOI: 10.1021/acs.inorgchem.6b00374
Inorg. Chem. 2016, 55, 7341−7355

py, pz,[19,77] and ac-py, CH_3CN[24]), *mer*-$[Ru(NH_3)_3(bpyam)(pz)](PF_6)_2$,[19] $[Ru(bpy)(Am)_4](PF_6)_2$ ($(Am)_4 = (NH_3)_4$ and $(en)_2$),[21,87,88] and $[Ru(bpy)_2(NH_3)_2](PF_6)_2$.[89] The complexes with MDA ligands used in this work are illustrated in Figure 2.

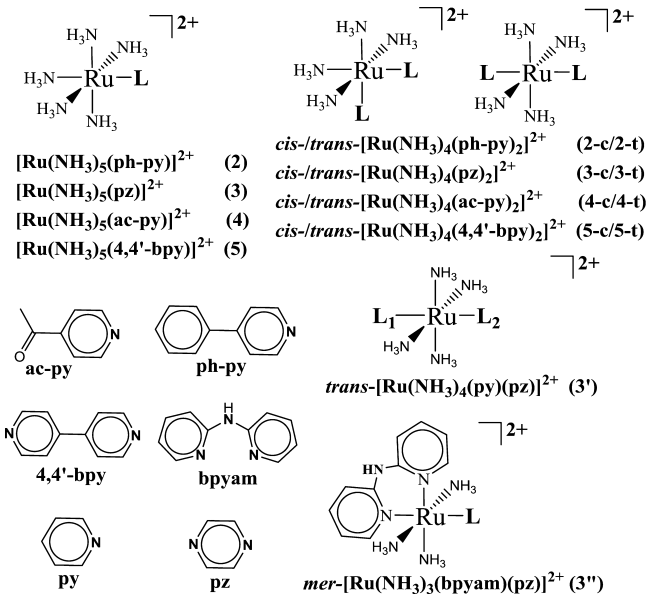

Figure 2. Ruthenium complexes with MDA ligands investigated in this work (code numbers have been chosen to be consistent with those in Tsai et al.[18]).

cis-/trans-[Ru(NH$_3$)$_4$(4,4′-bpy)$_2$](PF$_6$)$_2$ (5c/5t). A sample including 200 mg of *cis-/trans*-$[Ru(NH_3)_4(H_2O)_2](PF_6)_2$[77,78] and a 3 molar excess of 4,4′-bipyridine were added to 5 mL of degassed acetone under argon, and the mixture was stirred for 3 h at room temperature. The red solution was filtered, and the red acetone solution was mixed with 3 mL of saturated aqueous NH_4PF_6. The volume of the combined solutions was reduced to 3 mL and cooled in an ice bath. The resulting orange product was removed by filtration and washed with 2 mL of cold water, then by cold ether. The crude product was dried under vacuum conditions. Yield: 150 mg (40%). The crude product was purified by dissolving it in 1 mL of degassed acetone; this acetone solution was mixed with 5 mL of degassed aqueous NH_4PF_6 (1/10 of saturation). The volume of the resulting solution was reduced to 5 mL by rotary vacuum evaporation in an ice bath. The orange precipitate was removed by filtration and washed with 2 mL of cold water, then by cold ether. The product was dried under vacuum conditions. For *cis*-$[Ru(NH_3)_4(4,4'\text{-}bpy)_2](PF_6)_2\cdot(H_2O)_{2.5}$: Anal. calcd for $C_{20}H_{28}N_8P_2F_{12}Ru\cdot(H_2O)_{2.5}$: C, 29.37; N, 13.71; H, 4.07. Found: C, 29.44; N, 13.98; H, 3.91. ^{1}H NMR (acetone-d$_6$): δ 2.95 (s, 6H), 3.27 (s, 6H), 7.79−7.83 (m, 8H), 8.72−8.77 (m, 8H). ^{13}C NMR (acetone-d$_6$): δ 121.40, 122.93, 143.49, 144.25, 151.53, 158.41. For *trans*-$[Ru(NH_3)_4(4,4'\text{-}bpy)_2]\cdot(PF_6)_2\cdot(H_2O)_{2.5}$; Anal. calcd for $C_{20}H_{28}N_8P_2F_{12}Ru\cdot(H_2O)_{2.5}$: C, 29.37; N, 13.71; H, 4.07. Found: C, 29.36; N, 13.93; H, 4.37. ^{1}H NMR (acetone-d$_6$): δ 2.84 (s, 12H), 7.87 (d, J = 5.9 Hz, 4 H), 7.97 (d, J = 6.3 Hz, 4 H), 8.77 (d, J = 5.9 Hz, 4 H), 9.07 (d, J = 6.3 Hz, 4 H). ^{13}C NMR (acetone-d$_6$): δ 120.81, 122.57, 123.73, 149.67, 151.01, 156.85.

Instrumentation. The electrochemical measurements were performed using an Epsilon Electrochemical Workstation. Cyclic voltammograms (CV) and differential pulse voltammograms (DPV) were obtained in acetonitrile solution, which contained 10^{-3} M complex and 0.1 M *n*-tetrabutylammonium hexafluorophosphate (TBAH) at scan rates of 100 mV/s and 4 mV/s, respectively. Details have been reported previously.[18]

The 298 K absorption spectra in the solution of CH_3CN were determined with a Shimadzu UV-3101PC spectrophotometer. Absorption spectra in 87 K butyronitrile glasses were obstained as described in detail elsewhere[19] using a calibrated Xe line emission lamp for wavelength and an Oriel model 63966 Quartz Tungsten Halogen QTH lamp for intensity. A QTH lamp was also used as the light source in the determination of 87 K absorption spectra for the emission yield measurements. A P/N 21530 Specac variable temperature cell (−190 to 250 °C) with a square 1 cm quartz cuvette was used in the controlled-temperature cell holder with liquid or glass samples. The detection system contained a motor-driven Jobin-Yvon H-10 Vis monochromator, a Hamamatsu R928 phototube with a Jobin-Yvon (JY) PMT-HVPS power supply, a JY Spectracq2 for data acquisition, and the JY SynerJY software for data acquisition and data analysis.

Emission spectra and lifetimes in 77 K glasses were obtained in 2 mm i.d. cylindrical quartz cells in a spectroscopic quartz Dewar as described in detail elsewhere.[17,19] Emission spectral wavelengths were calibrated with the Xe lamp (Xe emission lines for wavelength and an Oriel model 63358 or 63966 Quartz Tungsten Halogen QTH lamp for intensity). The 77 K emission lifetimes were determined using Spectra Physics VSL-337ND-S nitrogen laser-pumped DUO-210 Dye laser system for excitation and a Hamamatsu P9220 PMT/E717−63 socket assembly mounted on a Jobin-Yvon H-100 spectrometer. Some of the 77 K emission lifetimes were determined using a Spectra Physics VSL-337ND-S nitrogen laser-pumped DUO-210 Dye laser system with a Hamamatsu NIR-PMT Model H10330A-75 detector and a National Instruments NI PCI-5154, 2 GS/s, 1 GHz Digitizer w/8 MB/ch onboard memory PC card as described previously[16,19,24]

^{1}H NMR (300 MHz) and ^{13}C NMR (75 MHz) spectra were determined using a Bruker AC-300 MHz spectrometer. All NMR spectra in this work were determined at ambient temperature using the solvent d_6-acetone. Chemical shifts (δ) in ppm were referenced to the solvent residual peak (d_6-acetone) as an internal standard, δ 2.04 for ^{1}H NMR and δ 29.84 for ^{13}C NMR spectra. Elemental analyses (C, N, H) were carried out on a Elementar Vario EL cube at the Instrumentation center of National Taiwan University.

Techniques. Relative emission yields in 77 K glasses were obtained using $[Ru(bpy)_3]^{2+}$ as the reference, as described in detail elsewhere.[19] See the Supporting Information for details. $[Ru(bpy)_3]^{2+}$, $[Os(bpy)_3]^{2+}$, and/or $[Ru(bpy)_2(en)]^{2+}$ in 77 K ethanol/methanol glasses were used as references for the determination of emission quantum yields (for excitation at both λ = 470 and 532 nm); the quantum yields reported for these complexes are $\phi_{(em)r} \approx 0.38$,[90−92] 0.038,[90−92] and 0.022,[91] respectively. Equation 7 was used to calculate the relative quantum yield of the target complex ($\phi_{(em)tc}$):[90,91]

$$\frac{\phi_{(em)tc}}{\phi_{(em)r}} = \frac{\eta_{tc}^2 I_{tc}}{\eta_r^2 I_r} \times \frac{1 - 10^{-A_r}}{1 - 10^{-A_{tc}}} \approx \frac{I_{tc} A_r}{I_r A_{tc}} \qquad (7)$$

where I_{tc} and I_r are the integrated areas under the emission spectra of the target complex (tc) and reference (r), respectively, A_{tc} and A_r are the absorbances of interest, respectively, η is the refractive index of the solvent, and $(\eta_{tc}^2/\eta_r^2) = 1$ in the same solvent system. We used cylindrical 2 mm i.d. fluorescence cells immersed in a Dewar with liquid nitrogen for the 77 K emission yield determinations. The sample path length for the absorbance in eq 7 varies from 0 to 1 for these cells, but the effective pathlengths did not vary much since the cell geometry and position were the same for the sample and reference solutions. High concentrations, [Ru-MDA] > 10^{-5} M, had to be employed with very weakly emitting substrates (for absorbances of about 1 in 1 cm), but in the 2 mm cylindrical cells, this amounts to an average absorbance of much less than 0.2 in the sample solutions. The target complexes were irradiated in their MLCT absorption bands by the most appropriate of the following diode laser modules: a 532 nm (30 mW) and a 470 nm (15 mW) CW MGL-S-B (Changchun Industries Optoelectronics Tech Co. Ltd.).

Values of k_{RAD} and k_{NRD} are obtained from $\phi_{(em)tc}$ and eqs 2 and 3 based on the assumption that the emitting states are formed with approximately unit efficiency ($\gamma \approx 1.0$) and that the lowest energy metal centered excited states (^{3}MC) have energies greater than that of ^{3}MLCT so that $k_{IC} \ll (k_{RAD} + k_{NRD})$. The relative energies of ^{3}MC

DOI: 10.1021/acs.inorgchem.6b00374
Inorg. Chem. 2016, 55, 7341−7355

Table 1. Ambient Absorption, 77 K Emission, Emission Decay Constants, and Emission Yield of the Ru-MDA Complexes[a]

			77 K emission properties in butyronitrile (alcohol) glass					
code	complexes	$h\nu_{max}$(abs)[b]	$h\nu_{max}$[b]	$h\nu_{ave}$[b,c]	k_{obs}, μs^{-1}[d]	$\phi_{em} \times 10^4$[e]	k_{RAD},[f] ms^{-1}	k_{NRD},[g] μs^{-1}
2	$[Ru(NH_3)_5(ph\text{-}py)]^{2+}$[h]	22.32 (21.93)	13.02 (12.3)	12.51 (12.3)	1.8 (4.4)	4.4 ± 0.4 (0.7 ± 0.2)	0.8 ± 0.1 (0.3 ± 0.1)	1.8 (4.4)
3	$[Ru(NH_3)_5(pz)]^{2+}$[h]	21.81	11.72	11.33	15	0.5 ± 0.2	0.7 ± 0.3	15
4	$[Ru(NH_3)_5(ac\text{-}py)]^{2+}$[h]	19.80	10.02	9.93	29	< 0.5	< 1.5	29
5	$[Ru(NH_3)_5(4,4'\text{-}bpy)]^{2+}$[h]	21.05	11.46	11.24	8.3	1.1 ± 0.4	0.9 ± 0.3	8.3
2-c	*cis*-$[Ru(NH_3)_4(ph\text{-}py)_2]^{2+}$[i]	22.15 (21.74)	14.8 (14.61)	13.86 (13.70)	0.37 (0.68)	130 ± 30 (42 ± 12)	4.8 ± 1.1 (2.8 ± 0.8)	0.37 (0.68)
2-t	*trans*-$[Ru(NH_3)_4(ph\text{-}py)_2]^{2+}$[i]	21.38 (20.96)	14.63 (14.52)	13.72 (13.47)	0.29 (0.75)	35 ± 5 (14 ± 4)	1.0 ± 0.2 (1.1 ± 0.3)	0.29 (0.75)
3-c	*cis*-$[Ru(NH_3)_4(pz)_2]^{2+}$[i]	21.98 (21.05)	13.50 (13.11)	12.75 (12.52)	3.6 (11)	14 ± 5 (5.1 ± 1.5)	5.0 ± 1.8 (5.5 ± 1.7)	3.6 (11)
3-t	*trans*-$[Ru(NH_3)_4(pz)_2]^{2+}$[i]	21.34 (20.49)	14.22 (13.08)	13.59 (12.53)	1.5 (20)	15 ± 5 (1.9 ± 0.6)	2.3 ± 0.7 (3.8 ± 1.2)	1.5 (20)
4-c	*cis*-$[Ru(NH_3)_4(ac\text{-}py)_2]^{2+}$[i]	19.86 (19.16)	12.62 (12.37)	11.99 (11.66)	6.7 (16)	6.0 ± 1.2 (1.5 ± 0.4)	4.0 ± 0.8 (2.4 ± 0.7)	6.7 (16)
4-t	*trans*-$[Ru(NH_3)_4(ac\text{-}py)_2]^{2+}$[i]	19.32 (18.66)	11.94 (11.56)	11.52 (11.53)	9.1 (17)	1.4 ± 0.3 (0.5 ± 0.2)	1.3 ± 0.3 (0.9 ± 0.4)	9.1 (17)
5-c	*cis*-$[Ru(NH_3)_4(4,4'\text{-}bpy)_2]^{2+}$	20.96 (20.24)	12.98 (12.78)	12.60 (12.38)	1.5 (6.2)	19 ± 2 (3.4 ± 1.0)	2.9 ± 0.3 (2.1 ± 0.6)	1.5 (6.2)
5-t	*trans*-$[Ru(NH_3)_4(4,4'\text{-}bpy)_2]^{2+}$	20.32 (19.59)	13.30 (12.76)	12.65 (12.23)	1.3 (4.1)	6.3 ± 1.1 (0.8 ± 0.2)	0.8 ± 0.2 (0.3 ± 0.1)	1.3 (4.1)
3′	*trans*-$[Ru(NH_3)_4(py)(pz)]^{2+}$[i]	21.76 (21.05)	12.92 (12.47)	12.80 (11.92)	2.9 (16)	3.2 ± 0.9 (0.5 ± 0.2)	0.93 ± 0.25 (0.8 ± 0.4)	2.9 (16)
3″	*mer*-$[Ru(NH_3)_3(bpyam)(pz)]^{2+}$[i]	21.80 (21.05)	13.67 (14.90)	13.36 (13.50)	1.9 (7.1)	8.5 ± 1.0 (6.7 ± 1.1)	1.6 ± 0.2 (4.8 ± 0.8)	1.9 (7.1)

[a]Dominant RT low-energy absorption maxima, $h\nu_{max}$(abs), determined in acetonitrile (alcohol); emission maxima, $h\nu_{max}$(em), mean excited state decay rate-constant, k_{obs}, and emission yield, ϕ_{em}, determined at 77 K in butyronitrile (alcohol) glasses; complex concentrations were in the 10^{-4} to 10^{-5} M range. [b]Energies in $cm^{-1}/10^3$. [c]$\nu_{ave} \approx (\int \nu_m I_m \, d\nu_m)/(\int I_m \, d\nu_m)$. [d]Mean excited-state decay rate constant, $k_{obs} = 1/\tau_{obs}$; uncertainty in k_{obs} is less than or equal to about 5% for each complex. [e]Emission quantum yield. [f]$\phi_{em} \times k_{obs}$; assumes $\gamma = 1$ in eq 1. [g]$k_{NRD} = k_{obs} - k_{RAD}$. [h]Ref 18. [i]Ref 19.

and ^{3}MLCT have been assessed by means of computational modeling and reported previously.[18]

Computational Details. Density functional theory[93] calculations have been performed to generate the triplet PE surfaces of the Ru complexes. The calculations have been done with a development version of Gaussian[93] with the B3PW91 functional[94−96] and the SDD basis set and pseudopotential[97] for the metal and 6-31G(d) basis[98,99] for the lighter atoms. Hydrogen bonding interactions between the Ru complexes and methanol molecule were calculated with 6-31G(d,p) basis sets instead of 6-31G(d) for lighter atoms. Solvation effects (in acetonitrile and ethanol) were accounted for using the implicit SMD solvation model[100] and were included during structure optimization. Wave functions were tested for SCF stability,[101−103] and all of the optimized structures were confirmed as minima by analyzing the harmonic vibrational frequencies. The ground singlet and triplet states were computed using the standard SCF method, and analytical frequencies were obtained for each. The isodensity plots (isodensity value 0.05 au) of the canonical and corresponding orbitals were visualized using GaussView.[104]

RESULTS

The emission spectra and lifetimes of these complexes have been reported elsewhere.[18,19] The relative quantum yields, ϕ_{em}, and emission decay rate constants, k_{obs}, for the target Ru-MDA chromophores in 77 K glasses are summarized in Table 1. In principle, the relative quantum yields obtained based on eq 1 should be corrected for the efficiency of populating the emitting state (γ). However, values of $\gamma \approx 1.0$ have been reported for $[Ru(bpy)_3]^{2+}$,[105] and we have been unable to find evidence for values of $\gamma \ll 1$ in this or in other recent work on Ru-bpy chromophores.[24] Consequently, we use $\gamma \approx 1.0$ in our analysis of the quantum yield data. See the Discussion section below for additional comments on this issue. The quantum yields are consistently smaller in alcohol than in butyronitrile. This appears to be mostly an effect of k_{NRD}, and in large part it arises from the smaller emission energies in the alcohol solvent (see also the Discussion below).

The observed emission decay rate constants can most simply be represented as in eqs 1−3, for these systems where k_{IC} usually corresponds to the internal conversion of an emitting ^{3}MLCT to a ^{3}MC excited state. In the limit that $\gamma = 1$ and $(k_{RAD} + k_{NRD}) \gg k_{other}$, the values of k_{RAD} and k_{NRD} can be readily evaluated, and such values have been assembled in Table 1. The excited state energy dependence of k_{RAD} is much smaller than found for the Ru-bpy chromophores,[24] and this comparison is developed in the Discussion below.

We have found anomalously large values of k_{NRD} for the complexes with Ru-pz and Ru-(ac-py) chromophores in the 77 K alcohol glasses (see Table 1 and Figure 8 in the Discussion section); some reasons that this behavior is unusual are noted in the Discussion section below. In order to gain some insight into this behavior, we have examined the acid dependent 300 K absorption and 77 K emission spectra of the *trans*-$[Ru(NH_3)_4(py)(pz)]^{2+}$ and *trans*-$[Ru(NH_3)_4(pz)_2]^{2+}$ complexes, and the 87 K absorption spectra of *trans*-$[Ru(NH_3)_4(py)(pz)]^{2+}$. Our observations are summarized in Figures 3 and 4 and in Table 2.

The MLCT excited states of complexes with Ru-pz and related chromophores are well-known to be more basic than their ground states;[79,106] however, the excited state basicities of these complexes are orders of magnitude smaller than those of the alkoxy anions at least at 300 K, and DFT modeling indicates that the base forms of the Ru-pz and Ru-(ac-py) complexes have no special affinity for the alcohol solvent (Supporting Information Table S9). The data in Table 2 are the experimental parameters characteristic of these complexes in

DOI: 10.1021/acs.inorgchem.6b00374
Inorg. Chem. 2016, 55, 7341−7355

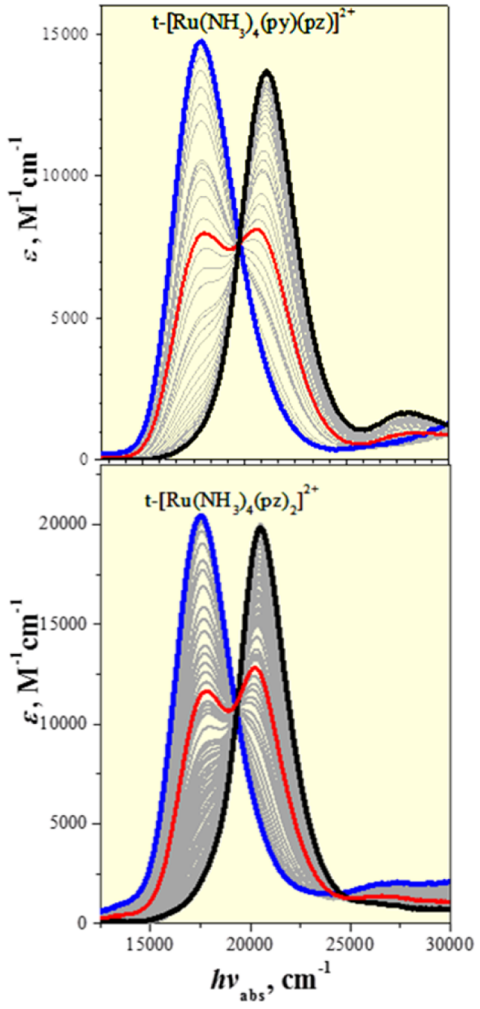

Figure 3. Changes in the ambient absorption spectra of Ru-MDA complexes with added acid: spectra of *trans*-$[Ru(NH_3)_4(py)(pz)]^{2+}$, upper panel, and *trans*-$[Ru(NH_3)_4(pz)_2]^{2+}$, lower panel, with variations in the concentrations of HOTf in ethanol/ methanol (4:1) solutions. The total concentrations of the Ru complexes were in the range of $(3.8–6) \times 10^{-4}$ M. In the upper panel, the added HOTf concentrations vary from [HOTf] = 0, black line, through [HOTf] = 1.17×10^{-1} M, red line, to [HOTf] = 8.73×10^{-1} M, blue line. In the lower panel, the added HOTf concentrations vary from [HOTf] = 0, black line, through [HOTf] = 2.54×10^{-1} M, red line, to [HOTf] = 1.01 M, blue line. The black lines correspond to the spectra of the parent $[Ru\text{-}pz]^{2+}$ complexes (base form, [HOTf] = 0) and the blue lines to the spectra of the $[Ru\text{-}pzH]^{3+}$ complexes (acid form, [HOTf] = upper limit). The red lines correspond to $[Ru\text{-}pz]^{2+}/[Ru\text{-}pzH]^{3+}$ = 1:1 (equivalence point); the relative acid dissociation constants, K_a' can be based on the excess HOTf concentration at this point: $K_a' = 3.0 \times 10^3$ for *trans*-$[Ru(NH_3)_4(py)(pz)]^{2+}$ and $K_a' = 1.7 \times 10^4$ for *trans*-$[Ru(NH_3)_4(pz)_2]^{2+}$. $K_a' = [[Ru\text{-}pz][HOTf]/[OTf^-][Ru\text{-}pzH^+]$.

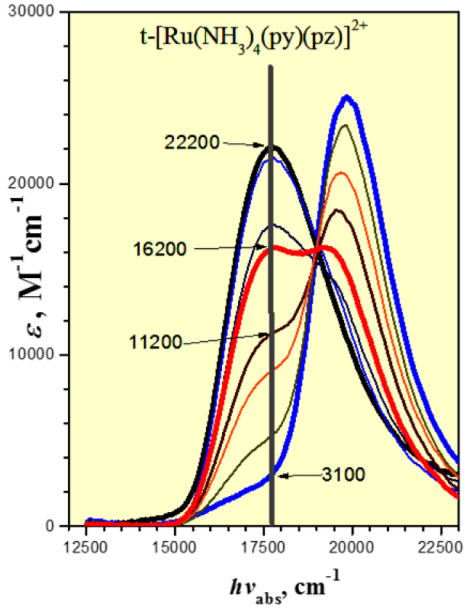

Figure 4. Changes in the 87 K absorption spectra of *trans*-$[Ru(NH_3)_4(py)(pz)]^{2+}$ with variations in the concentrations of HOTf in ethanol/methanol (4:1) glassy solutions. The added HOTf concentrations vary from [HOTf] = 0, blue line, through [HOTf] = 3.26×10^{-4} M, dark red curve, and [HOTf] = 4.66×10^{-4} M, red line, to [HOTf] = 1.165 M, black line. The apparent relative acid dissociation constant (K_a') is 21.9 at 87 K.

the alcohol media, and the differences in absorption maxima for the acidic and basic forms of the complexes imply that the excited states are far more basic than the ground states. However, the quantitative evaluation of this difference is not altogether straightforward. Thus, the ground state values of $K_a' = K_a[HOTf]/[OTf^-][H^+] > 1$, which indicate that HOTf is a weaker acid in this medium than are the protonated pyrazine complexes. The absorbance shift to lower energies for the protonated pyrazine complexes indicates that the Ru-pz excited states are much stronger bases than their ground states, nominally by a factor on the order of 10^7 for ambient solutions. However, the excited states generated by absorption are Franck–Condon (FC) excited states with ground state nuclear coordinates and lifetimes in the femtosecond regime, so that they cannot be in equilibrium with the bulk medium. This is an even more serious issue since the observed absorption bands are generally the convolution of several electronic transitions ($S_0 \rightarrow S_n$, $n > 1$)[71,72] involving different nonequilibrium excited state electronic distributions[71,72] and consequently different solvation energies. Thus, the relative acid dissociation constants, K_e(FC), inferred from the differences in absorption of the acid (RH^+) and basic (R) forms of a substrate (see Figure 5) are not equilibrium constants and only qualitatively useful. Similarly, the negligible diffusion of molecular species in glasses make the 87 K value of K_a in Table 2 only qualitatively useful. Nevertheless, the sizable shifts to lower energy absorption upon protonation of the complexes in ambient solution and 87 K (Table 2) indicates that the excited states are much more basic than the ground states (see similar conclusion by Ford et al.[79]). The magnitude of this shift implied by the data in Table 2 is (based on the quasi-thermodynamic cycle implied in Figure 5) $K_a' \sim 10^{-13}$. The initial amplitudes observed in the emission decay rate constants in Table 3 imply a somewhat smaller value of K_a' at 77 K.

Although the emissions of the equilibrated triplet excited state, T_0, to the ground state, S_0, are generally less complicated electronically than the absorptions, similar considerations should apply to the evaluation of the triplet state basicities, $K_e(T_0)$, but we have been unable to detect emissions from the Ru-pzH^+ species. These considerations suggest that long-range 77 K proton transfer is restricted by solvent reorganizational barriers of greater than $2k_BT$ (or about 300 cal/M). The apparent differences between K_a' at 87 and 77 K may arise from nearest neighbor proton transfer only with the HOTf in the

DOI: 10.1021/acs.inorgchem.6b00374
Inorg. Chem. 2016, 55, 7341–7355

Table 2. Absorption Data for Titrations with HOTf

complex	T	$h\nu_{max}$,[a] $cm^{-1}/10^3$ (ϵ_{max}, cm^{-1} $M^{-1}/10^3$) base form (B)	$h\nu_{max}$,[a] $cm^{-1}/10^3$ (ϵ_{max}, cm^{-1} $M^{-1}/10^3$) acid form (BH^+)	$[HOTf]_{1/2}$,[b] M	K_a'[c]
trans-$[Ru(NH_3)_4(py)(pz)]^{2+}$	298 K	21.1 (13.8 ± 0.2)	17.9 (15.0 ± 0.2)	0.12 ± 0.01	2700 ± 300
	87K	19.5 (25.0)	17.7 (22.2)	3.7×10^{-4}	21.9[d]
trans-$[Ru(NH_3)_4(pz)_2]^{2+}$	298 K	20.5 (21.2 ± 0.8)	17.5 (21.7 ± 0.8)	0.21 ± 0.03	14000 ± 2000

[a]Absorption maxima in ethanol/methanol. [b]$[HOTf]_{1/2}$ is the acid concentration at $[B] = [BH^+]$. [c]Calculated at the equivalence point as $K_a' = ([B]_{1/2}[HOTf]_{1/2})/([BH^+]_{1/2}[OTf^-]_{1/2})$ and $[B]_{1/2} = [BH^+]_{1/2} = [OTf^-]_{1/2}$, where $[BH^+]_{1/2}$, $[HOTf]_{1/2}$, and $[B]_{1/2}$ are the concentrations at $[B] = [BH^+]$; note that this differs from the conventional definition of the acid dissociation constant, $K_a(BH) = ([B]_{1/2}[H^+]_{1/2})/([BH^+]_{1/2})$, since acids are expected to be weaker in nonaqueous media. [d]This probably does not correspond to an actual equilibrium distribution of species at 87 K.

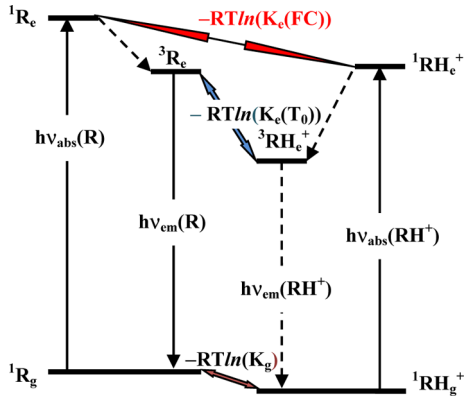

Figure 5. Qualitative energy level diagram illustrating the relationships between electronic states of the acid and base forms of a substrate. For brevity, we have represented the base form of the complexes as R_x and the acid form as RH_x^+ (x = g or e for the ground state and the Franck–Condon excited state, respectively). Note that there is no simple pathway connecting the two Franck–Condon excited states, ^1R_e and $^1RH_e^+$.

Table 3. Acid Dependence of *trans*-$[Ru(NH_3)_4(py)(pz)]^{2+}$ 77 K Lifetimes for Various [HOTf] in Alcohol Glasses[a]

[Ru-pz] (M)	[HOTf] in alcohol (M); {[HOTf]/[Ru-pz]}[b]	avg. 77 K lifetime, *ns* (A_{ini})[c]
4.31×10^{-4}	0	69 ± 2 (2.53)
5.39×10^{-4}	1.1×10^{-3} {2.0}	70 ± 1 (2.44)
3.77×10^{-4}	1.32×10^{-3} {3.5}	62 ± 1 (1.83)
4.85×10^{-4}	1.65×10^{-3} {3.4}	59 ± 1 (0.85)
5.93×10^{-4}	2.2×10^{-3} {3.7}	59 ± 1 (0.97)
5.93×10^{-4}	5.5×10^{-3} {9.3}	59 ± 1 (0.69)
4.85×10^{-4}	1.1×10^{-2} {23}	75 ± 3 (0.18)
3.77×10^{-4}	1.65×10^{-2} {44}	70 ± 1 (0.22)
4.85×10^{-4}	1.1×10^{-1} {227}	78 ± 3 (0.12)[d]

[a]The lifetime measurements were performed using a Hamamatsu NIR-PMT Model H10330A-75 with 483 nm nitrogen-pumped dye laser excitation; ethanol/methanol = 4:1 (v/v′); A_{ini} = average initial amplitude at $t = 0$ for the emission decay. [b]Ratios between [HOTf] and [Ru-pz]. [c]Average of single exponential fit of the emission decay amplitude by origin 8.0; A_{ini} = average of the initial ($t = 0$) emission decay curve amplitudes, for 3–10 decays. [d]Partly convoluted with instrument response.

first few solvation shells of the complex contributing and bulk acid concentration being frozen.

Despite the strong acid dependence of the 77 K emission intensities, the emission decays of $[Ru(NH_3)_4(py)(pz)]^{2+}$ were acid independent, single exponential decays (see Table 3): $k_{obs}(ave) = (67 \pm 7)$ ns^{-1} with $0 \le [HOTf]/M \le 0.1$.

On the basis of our observations, it is clear that, for a given $[H^+]$, the ratio of basic to acidic forms of the ^{1}MLCT excited states of the *trans*-$[Ru(NH_3)_4(py)(pz)]^{2+}$ complex decreases dramatically with temperature as is common for weak acids.[107] The distribution of R_g and RH_g^+ ground state species is well-defined in fluid solution, but equilibrium cannot exist between the acidic and basic forms of the complex and the added acid in the bulk frozen solution. On the basis of the correlation of Ru-MDA spectral absorption and emission maxima (Figure 3 in Tsai et al.),[18] the maximum for this emission is predicted to occur at about 9000 ± 400 cm^{-1} (about 1100 nm), and based on the variations of k_{NRD} with excited state energy (discussed below), the emission lifetime would be less than about 10 ns, which would be difficult for us to detect. Since the excited state lifetimes are nearly [HOTf] independent and consistent with detection of emission from only the basic form of the complex at 77 K, while the decay amplitudes are acid dependent, the rate constant for proton quenching of the excited state (k_Q in eq 8) cannot contribute to the observed excited state decay rate constant (k_{obs}) even in the acidic solutions or to k_{NRD} in the neat alcohol solutions.

$$^3MLCT + H^+ \begin{cases} \rightarrow \text{Ru-BH}^+, k_Q \\ \rightarrow \text{Ru-B}, k_{obs} \end{cases} \quad (8)$$

The results of our DFT modeling are summarized for α-orbital SOMOs in Figure 6 and in Table 4; the α- and β-orbital contribution to the ^{3}MLCT frontier orbitals are presented in the Supporting Information, Figures S7 and the corresponding orbitals in Figure S8.[108] Table 4 shows that the $d\pi(Ru)-\alpha$-orbital SOMOs have considerable contributions from a ligand(A)-based π molecular orbital, while the ligand(A)-centered, $\pi^*-\alpha$-SOMO has negligible contribution (0–2%) from a $d\pi(Ru)$ orbital. The bpy-based π-MO contribution to the $d\pi(Ru)$ α-SOMO of the $[Ru(NH_3)_4(bpy)]^{2+}$ complex is much larger (about 45%) than the MDA-based π-MO contributions to the $d\pi(Ru)-$SOMOs of the Ru-MDA chromophores (about 10–30%). This illustrates that the ^{3}MLCT state of the Ru-bpy complex has significantly more $d\pi(Ru)-p\pi(A)$ mixing than the ^{3}MLCT states of the Ru-MDA complexes. This can arise from a large difference in the energies and/or the magnitudes of the spatial overlap of the interacting $d\pi(Ru)-$SOMO and π-MO of the aromatic ligand. Larger spatial $d\pi(Ru)-p\pi(A)$ overlap is likely in the Ru-bpy chromophores since (1) it involves an interaction of the *two* $p\pi$-orbitals at the bpy-nitrogen atoms with the Ru-d_{xy} orbital and (2) the orbital (see Figure 6) and electron[18] density in π-MO of $[Ru(NH_3)_5(ph\text{-}py)]^{2+}$ is distributed over two aromatic rings, reducing the effective overlap parallel to the *single* MDA–

DOI: 10.1021/acs.inorgchem.6b00374
Inorg. Chem. 2016, 55, 7341–7355

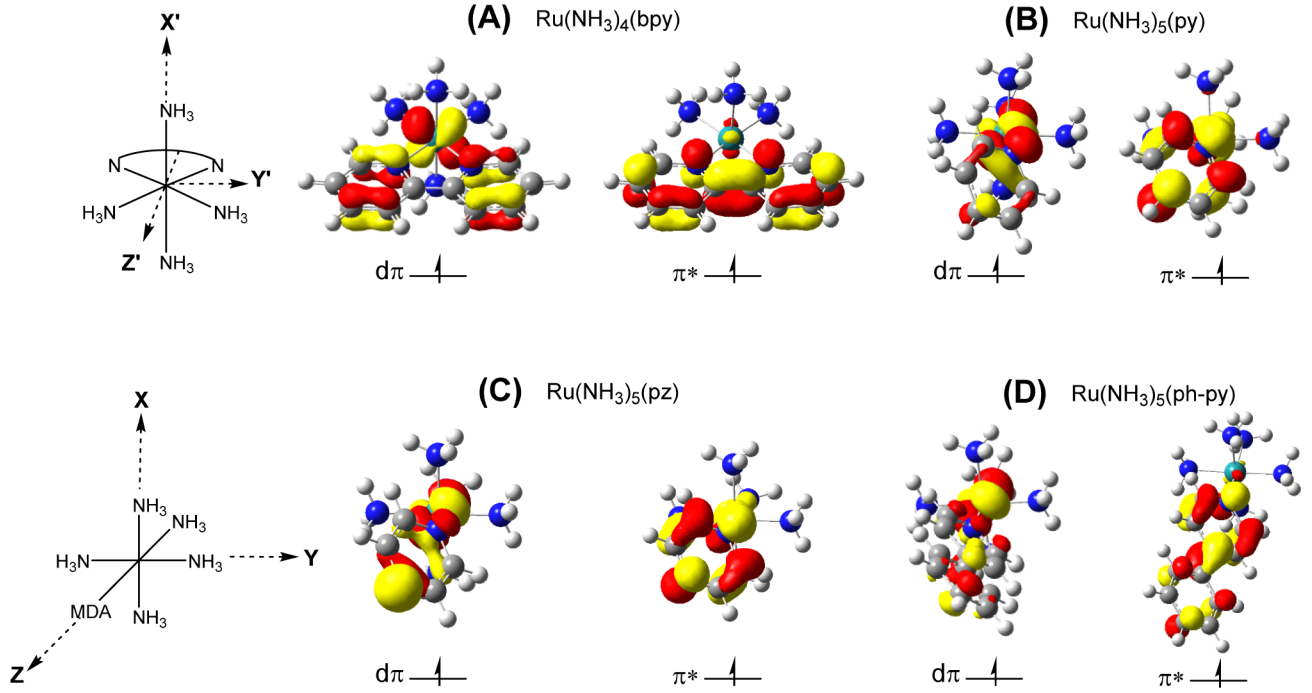

Figure 6. Alpha components of the singly occupied dπ(Ru) molecular orbitals (dπ–SOMO) and ligand (A)-based π* molecular orbitals (π*–SOMO) of the ^{3}MLCT states of (A) $[Ru(NH_3)_4(bpy)]^{2+}$ and three Ru-MDA complexes: (B) $[Ru(NH_3)_5(py)]^{2+}$, (C) $[Ru(NH_3)_5(pz)]^{2+}$, and (D) $[Ru(NH_3)_5(ph\text{-}py)]^{2+}$. Note that different Cartesian axes are used for Ru-MDA and $[Ru(NH_3)_4(bpy)]^{2+}$: in the former, the *z* axis is coincident with the Ru-N(MDA) bonding axis, but this is not the case for the latter. The Ru-MDA complexes display a poorer spatial overlap between the dπ(Ru) and ligand (A) π molecular orbitals compared to that by the Ru-bpy complex. Note that the *y*- and *z*-coordinate axes of $[Ru(NH_3)_4bpy]^{2+}$ are rotated 45° with respect to the Ru–N bonding axes. Canonical orbitals are plotted with an isosurface value of 0.05 au.

Table 4. Relative α-Orbital Contributions[a] of dπ(Ru) and Ligand(A)-based σ and π Orbitals to the Metal-Centered SOMOs of the ^{3}MLCT States of $[Ru(NH_3)_4(bpy)]^{2+}$, $[Ru(NH_3)_5(py)]^{2+}$, $[Ru(NH_3)_5(pz)]^{2+}$, and $[Ru(NH_3)_5(ph\text{-}py)]^{2+}$

	dπ(Ru)–SOMO of ^{3}MLCT[a]		
complex	dπ(Ru) character	ligand (A)-based π character	ligand (A)-based σ character
$[Ru(NH_3)_4(bpy)]^{2+}$	51%	45%	----
$[Ru(NH_3)_5(py)]^{2+}$	62%	31%	----
$[Ru(NH_3)_5(pz)]^{2+}$	59%	9%	24%
$[Ru(NH_3)_5(ph\text{-}py)]^{2+}$	62%	32%	----

[a]The contribution from each relevant atom was calculated by summing the contributions of all basis functions of a given angular momentum.

Ru–NH_3 axis even more than in the py and pz complexes. Interestingly, as shown in Figure 6 and Table 4, the dπ(Ru)–SOMO of $[Ru(NH_3)_5(pz)]^{2+}$ displays a large contribution (about 24%) from a σ-MO on the pyrazine nitrogen atom that is not coordinated to Ru. This σ(metal–ligand) interaction arises due to the rotation of the pz ligand out of the Cartesian plane in the excited state, thereby facilitating the nominal pπ(pz)/dσ(Ru) overlap,[18,19] and it is pertinent to the observed larger basicity of the pz complex in its excited state compared to its ground state.

For clarity in the comparisons of dπ(Ru)–pπ(A) orbital overlap in the Ru-MDA and $[Ru(NH_3)_4(bpy)]^{2+}$ complexes, we label the Cartesian axes used for the latter as *x*′, *y*′, and *z*′ (where only *x*′ is coincident with a N–Ru–N bonding axis; see Figure 6) and reserve the unprimed notation for the Cartesian axes nearly coincident with the N–Ru–N bonding axes. In the calculated ^{3}MLCT $[Ru(NH_3)_4(bpy)]^{2+}$ excited state structure in Figure 6, the singly occupied dπ–SOMO is similar to a $d_{x'y'}$(Ru) orbital (a symmetry adapted combination of d_{xz} and d_{xy} orbitals), and the bpy ligand is coplanar with the amine ligands in the *y*′*z*′ plane. In contrast, the aromatic ligands of ^{3}MLCT Ru-MDA complexes are folded between the Cartesian *xz* and *yz* planes, and the interacting dπ–SOMO also has a spatial distribution that is between the NH_3–Ru–NH_3 axes (approximately a combination of d_{xz} and d_{yz} orbitals) and appropriate for overlap with a π-MO of the aromatic ligand.

DISCUSSION

We have now examined the emission spectra,[18] excited state lifetimes,[18] and quantum yields for a substantial number of complexes with Ru-MDA chromophores, and these provide an instructive contrast with the previously reported emission properties of Ru-bpy chromophores.[20,21,24] The 77 K emission intensities and relative sideband amplitudes of complexes with Ru-MDA chromophores are much weaker and vary much less in relative amplitude than do those of the Ru-bpy chromophores in the same range of energies.[18,19] This contrast in sideband amplitudes contradicts the qualitative expectation that an electron in the LUMO of a single aromatic ring of the MDA acceptor ligand will lead to a more distorted ligand structure than when this charge is spread over the two rings of the bpy ligand. Similarly, resonance-Raman data for the *trans*-$[Ru(NH_3)_4(ac\text{-}py)_2]^{2+}$ and $[Ru(NH_3)_4bpy]^{2+}$ complexes imply greater vibronic amplitudes in the former (see Supporting Information Tables S3 and S4).[84,109] The resolved nonradiative (k_{NRD}) and radiative (k_{RAD}) decay rate constants of the Ru-MDA chromophores in butyronitrile and a 4 to 1 mixture of

DOI: 10.1021/acs.inorgchem.6b00374
Inorg. Chem. 2016, 55, 7341–7355

ethanol and methanol provide some unique perspectives on the excited state properties of transition metal complexes and help resolve the noted issues concerning band shape differences. Our recent work indicates that most of the vibronic sideband structure observed for Ru-bpy chromophores with $h\nu_{max} \geq 13\,000$ cm^{-1} arises from configurational mixing with a higher energy-acceptor−ligand-centered excited state,[16] and for these complexes, this is accompanied by an excited state energy dependence of k_{RAD} over and above that indicated in eqs 3−6.[24] However, the present study has found no such "extra" excited state energy dependence for the Ru-MDA chromophores. Our DFT modeling indicates that there is considerable mixing between excited states and that this mixing is mediated by $d\pi(Ru)/p\pi(A)$ overlap, which is consistent with the energy dependence found for the vibronic amplitudes of Ru-bpy chromophores.[21,45,48,49,71−76] In contrast, there is no evidence for mixing between the triplet excited states and the ground states of the complexes examined (see the Supporting Information Figure S9).

The Franck−Condon excited states of transition metal complexes tend to relax very rapidly to the lowest energy excited state,[110] and most excited state chemistry and emission has been attributed to this state.[43,46−50] However, the ^{3}MLCT excited states of many Ru-A complexes emit in 77 K glasses even when detailed DFT modeling indicates that one or more ^{3}MC excited state has a lower energy.[17,19,24,111−113] On the basis of the DFT modeling, this "non-Kasha"[114] behavior does not appear to be an issue for the Ru-MDA complexes discussed here,[17,24] and there is no experimental evidence for significant k_{IC} contributions to k_{obs} at 77 K.[16,20] We have resolved k_{NRD} and k_{RAD} using the ϕ_{em} and k_{obs} values in Table 1. Small experimental values of the low-temperature emission yields for molecular excited states are most commonly attributed to $k_{obs} \gg k_{RAD}$, but in these ruthenium complexes, with their multitudes of possible excited states, there could be many different upper state relaxation channels, some of which might lead to different distributions of low energy ^{3}MLCT and ^{3}MC excited states and thereby lower the efficiency, γ, for populating the emitting state.[19] We have previously shown that the complexes with Ru-MDA chromophores have slightly longer 77 K emission lifetimes than do the Ru-bpy chromophores with the same ^{3}MLCT energy, and that there is little variation in the estimated energies of the lowest energy ^{3}MC excited states while the energies of the ^{3}MLCT excited states vary a great deal. Since there is no correlation of k_{obs} with the calculated differences between $E(^3MC)$ and $E(^3MLCT)$, it is unlikely that γ is much less than 1.[18] If γ were sufficiently small to account for the very small values of ϕ_{em}, then k_{RAD} would generally be more than 10^3-fold larger than the values in Table 1 (i.e., for γ = 1) leading to smaller k_{NDR} values than those presented in Table 1 and resulting in different patterns of the $h\nu_{ave}$[52] dependencies for the Ru-MDA and Ru-bpy chromophores, in contrast to that shown in Figure 7. Although we have no direct way to evaluate γ, the circumstantial evidence cited strongly supports the assumption that $\gamma \approx 1$. As noted above, the values of k_{obs} are somewhat smaller than those found for Ru-bpy chromophores with comparable energies. Since it appears that $k_{IC} < (k_{RAD} + k_{NRD})$ for these complexes, this must mean that k_{NRD} and/or k_{RAD} must be smaller than found for the Ru-bpy chromophores. Thus, the very small values of emission yields found for the Ru-MDA chromophores is most likely the result of a much smaller value of k_{RAD} for them than for the Ru-bpy chromophores. A more detailed account of these issues follows.

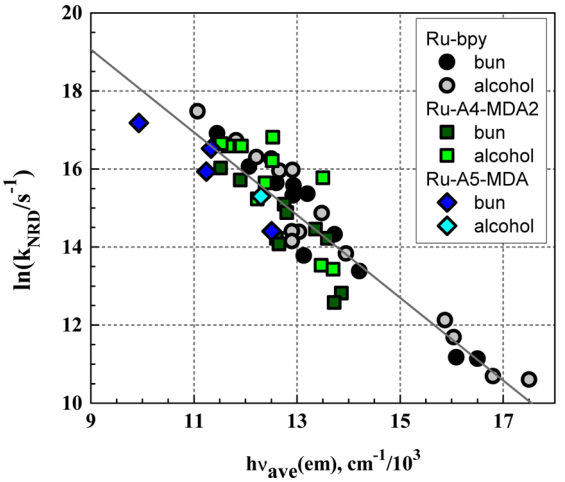

Figure 7. Correlation of k_{NRD}, resolved from ϕ_{em} (eqs 1−3, assuming $\gamma \approx 1$) with an $h\nu_{ave}$ of the 77 K emission for Ru-bpy and Ru-MDA chromophores (see inset). Emission data for Ru-bpy chromophores from Thomas et al.[24] and for Ru-MDA chromophores from Tsai et al.,[18] as summarized in Table 1. For all Ru-bpy and Ru-MDA complexes, the least-squares line has a slope of −1.06 ± 0.06 and an intercept of 28.6 ± 0.8 (r^2 = 0.84).

The Patterns of Nonradiative Decay in the Ru-MDA Chromophores. The 77 K excited state lifetimes of most of these complexes tend to be dominated by k_{NRD}. The apparent values of k_{NRD} for the Ru-MDA chromophores are slightly smaller (roughly 4-fold) than those of Ru-bpy chromophores with similar values of $h\nu_{ave}$; see Figure 7. The comparisons of k_{NRD} for the different chromophores can be represented more explicitly in terms of the relationship of k_{NRD} to excited state energy in the limit of a single distortion mode, $h\nu_h$:[50]

$$k_{NRD} \approx B\, e^{-\gamma_{EJ}(h\nu_{ave}/h\nu_h)} \quad (9)$$

with $B \approx (H_{e,g})^2[8\pi^3/(h^3\nu_h h\nu_{ave})]^{1/2}$, where we have substituted $h\nu_{ave}$ for $E^{0,0}$. Equation 9 assumes a single distortion mode of frequency ν_{vib} and is obtained from the Huang−Rhys parameter for the harmonic of this distortion mode whose energy approximates that of the excited state, $Nh\nu_h \approx h\nu_{ave}$, for which the Huang−Rhys factor is $(S_d)^N/N!$ ($S_d = \lambda_h/(h\nu_h)$) using a form of Stirling's approximation for the $N!$ term in the more general relaxation rate constant expression[50,51] (λ_h is the vibrational reorganizational energy associated with the distortion in ν_h and proportional to the distortion squared; $\gamma_{EJ} \approx [\ln(h\nu_{ave}/\lambda_h) - 1]$; other approximations are $h\nu_{ave} \gg h\nu_h$ and $h\nu_{ave} > \lambda_h$).[50] For a single distortion mode, γ_{EJ} is constant, and eq 9 is the basis for the correlation in Figure 7. However, this model is not quantitatively applicable to these systems since (a) there are many excited state distortion modes (more than 10) in these complexes;[84,109,115,116] (b) the similarities of k_{NRD} for the Ru-bpy and Ru-MDA chromophores in Figure 7 imply similar distortion mode energies ($h\nu_h$) and amplitudes (λ_h), whereas their rR parameters are different (see Supporting Information Tables S3 and S4);[84,109,115,116] and (c) eq 9 is not quantitatively compatible with the observations since assuming an equivalent averaged single distortion mode based on averaging *rR* parameters (see Supporting Information Tables S3 and S4)[84,109] results in a calculated value for $[Ru(NH_3)_4bpy]^{2+}$ that is larger than that for $[Ru(NH_3)_5(acpy)]^{2+}$ by a factor of 10^3−10^6 (depending on how the parameters are averaged), while the observed values of k_{NRD}

DOI: 10.1021/acs.inorgchem.6b00374
Inorg. Chem. 2016, 55, 7341−7355

(from eqs 2 and 3) for the latter are slightly smaller than those of the former at similar energies. The large number of distortion modes very likely leads to a multitude of vibronic decay channels, differing in their combinations of molecular distortion modes, leading to inconsistencies with the details of the single mode model. A more realistic model would replace the single decay channel represented in eq 10 by a sum over all possible channels; in its simplest, somewhat schematic form:

$$k_{NRD} \approx B \sum_{r}^{\text{all-channels}} \left[e^{-\gamma_{EJ}(h\nu_{ave}/h\nu_{h})}\right]_{r} \quad (10)$$

where γ_{EJ} and $h\nu_{h}$ are constructed from the different combinations of distortion modes in each channel. However, the number of possible decay channels is extremely large, and we do not currently have a way to handle this.

Table 5 illustrates in more detail the observed similarities of k_{NRD} in the 77 K alcohol and butyronitrile glasses for the Ru-bpy and Ru-MDA. The data set used for the Ru-MDA complexes in the alcohol solvent is relatively small, and as a consequence it is not clear whether the slightly steeper slope is significant. Otherwise, the parameters are statistically indistinguishable for a variety of different chromophores in the different solvents.

Table 5. Comparison of the Energy Dependences of k_{NRD} for Ru-MDA and Ru-bpy Chromophores in 77 K Glasses

		least squares fit for $\ln(k_{NRD}) = a \times h\nu_{ave} + b$		
chromophore	77 K glass	slope (a)	intercept (b)	r^2
Ru-MDA	Butyronitrile	−1.1 ± 0.1	28 ± 2	0.84
	Ethanol/Methanol[a]	−1.4 ± 0.2	33 ± 2	0.99
Ru-bpy[b]	Butyronitrile	−1.2 ± 0.1	30.5 ± 1.3	0.95
	Ethanol/Methanol	−1.1 ± 0.1	29 ± 1	0.94

[a]The Ru-pz and Ru-(ac-py) chromophores were omitted. [b]Data from Thomas et al.[24]

The values of k_{NRD} for some Ru-pz and Ru-(ac-py) chromophores determined in neutral alcohol glasses are significantly larger than those determined in butyronitrile glasses even for some Ru-bpy chromophores that are similar in energy. This is more evident when considering the k_{NRD} energy dependence for Ru-MDA complexes only as in Figure 8. This behavior is not consistent with eq 10 since the emission is from the basic forms of the complexes, and eq 10 tends to emphasize the highest frequency molecular distortion modes[50,51] which are independent of the solvent. The large excited state basicity might be invoked to account for the deviations of the Ru-pz and Ru(ac-py) complexes from the usual behavior in Figure 8, but our observations summarized in Tables 2 and 3 and the associated comments in the Results section show that we only observed emission from the basic form of these complexes: emission from the protonated complexes is not observed, and protonation of the complexes cannot account for the deviations. Although specific solvent contributions are not usually considered in treatments of k_{NRD} such as eq 10, we have examined the ^{3}MLCT excited state interactions of these complexes with methanol by means of DFT modeling, and there is no evidence for any base dependent association among the complexes (see Supporting Information Table S9). It is possible that the larger values of k_{NRD} observed for the Ru-pz and Ru-(ac-py) chromophores in alcohol glasses arise from a hydrogen bonding interaction with the solvent with very short times for the proton at the PE minimum near the basic moieties in the excited states.

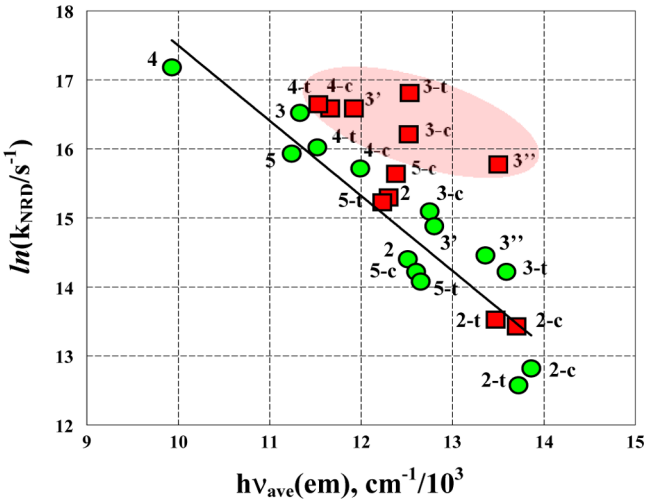

Figure 8. Correlation of k_{NRD}, resolved from ϕ_{em} (assuming $\gamma \approx 1$), with $h\nu_{ave}$ for the 77 K emissions for Ru-MDA chromophores in butyronitrile (green) and alcohol (red) glasses. The complexes with Ru-pz and Ru-(ac-py) chromophores in the alcohol glasses are surrounded by the red ellipse. The code numbers are from Table 1. The solid line is a least-squares fit to the data for Ru-MDA chromophores in butyronitrile (r^2 = 0.84): $\ln(k_{NRD}/s^{-1}) = -(1.1 \pm 0.1)h\nu_{ave} + (28 \pm 2)$.

Comparison of k_{RAD} Values for Ru-MDA and Ru-bpy Chromophores. The 77 K emission spectra of Ru-MDA complexes tend to be broad and structureless with little evidence for vibronic sideband contributions in contrast to the 77 K emission spectra of Ru-bpy. Our recent work has indicated that much of the vibronic sideband structure observed for Ru-bpy chromophores with $h\nu_{max} \geq 13\,000$ cm^{-1} arises from configurational mixing with a higher energy acceptor−ligand centered excited state,[16] and this is accompanied by an "extra" excited state energy dependence of k_{RAD} for these complexes.[24] However, no such "extra" excited state energy dependence has been found for the Ru-MDA chromophores. It is important to observe that the values of ϕ_{em} and $k_{RAD}/(h\nu_{ave})^3$ for Ru-bpy chromohores approach very small values for small values of $h\nu_{ave}$ (thus, large values of $\Delta E_{LL,CT}$) as indicated by the arrow in Figure 9.

The observations on Ru-MDA chromophores are considered in more detail in Figure 10 using an expanded energy scale. Figures 9 and 10 indicate that there is no "extra" energy dependence, and no intensity stealing, for Ru-MDA complexes over the available energy range, and this suggests that $^1\pi^1\pi^*/^1d_\pi{}^1\pi^*$ excited state/excited state configurational mixing does not significantly affect the Ru-MDA emission properties and therefore that the first term in eq 6 dominates in the energy range examined. Our computational modeling in Figure 6 and in Table 4 qualitatively illustrate that the dπ−SOMO/pπ(aromatic ligand HOMO) spatial overlap can be better for $[Ru(NH_3)_4(bpy)]^{2+}$ than for the Ru-MDA complexes in their vibrationally relaxed ^{3}MLCT states. As a result of the greater Ru/bpy than Ru/MDA mixing, $H_{CT,LL}$ is expected to be larger for the Ru-bpy ^{3}MLCT excited states than it is for the Ru-MDA ^{3}MLCT excited states.

Since the ^{3}MLCT → S_0 transition is forbidden in the absence of spin−orbit coupling, the SOC-promoted emissions should in

DOI: 10.1021/acs.inorgchem.6b00374
Inorg. Chem. 2016, 55, 7341−7355

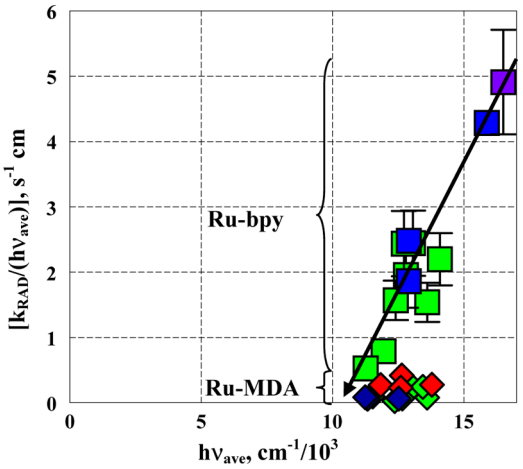

Figure 9. Contrasts in the variations in the apparent energy dependence of the 77 K emissions of Ru-bpy and Ru-MDA chromophores: $k_{RAD}/(h\nu_{ave}) \propto H_{e,g}^2$, based on eqs 4 and 6. For Ru-bpy: blue squares, for alcohol only (data of Demas and Crosby),[91] purple squares for butyronitrile only, and green squares for average of $h\nu_{ave}$ and $(k_{RAD}/h\nu_{ave})$ determined in alcohol and butyronitrile (data of Thomas et al.[24]). The diamonds are for Ru-MDA chromophores; more details in Figure 10. The error bars are based on either the replicate determinations of ϕ_{em} in a single solvent or the difference between determinations in the different solvents. Note that there is a possibility that $(\Delta\mu_{e,g})^2$ in eq 3 could be somewhat solvent dependent; this might contribute to the relatively large differences in values found for the smaller Ru-bpy chromophores (i.e., those with am(m)ine rather than bpy ancillary ligands).

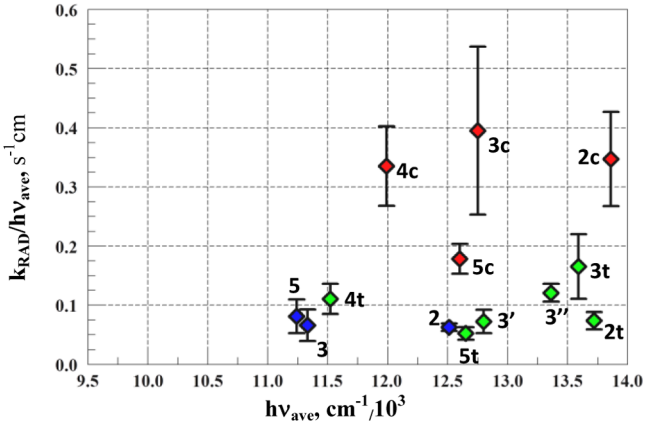

Figure 10. Variations in the apparent energy dependence of $k_{RAD}/(h\nu_{ave})$ for the 77 K emissions Ru-MDA chromophores (red, blue, and green points). Data are from Table 1; red for *cis*-$[Ru(NH_3)_4(MDA)_2]^{2+}$, green for *trans*-$[Ru(NH_3)_4(MDA)(MDA')]^{2+}$, and blue for $[Ru(NH_3)_5MDA]^{2+}$. The code numbers are from Table 1.

principle take account of all interactions between the triplet and singlet manifolds that might contribute to the relaxation of the spin constraint, and since the emitting ^{3}MLCT state appears to contain contributions from a higher energy $^3\pi\pi^*$ excited state, this also must be considered. Thus, the SOC interaction can be formulated in terms of a mixing matrix element (X = CT (for MLCT) or $\pi\pi^*$)

$$H_{^3X,n}^{SOC} = \langle \Psi_{^3CT}^{dia} + \alpha_{^3CT,^3\pi\pi^*} \Psi_{^3\pi\pi^*}^{dia} | H^{(SOC)} | \Psi_{^1S_n}^{dia} \rangle \quad (11)$$

SOC and intensity stealing require at least a five state model (with excited states as in Figure 11 and in contrast to Figure 1).

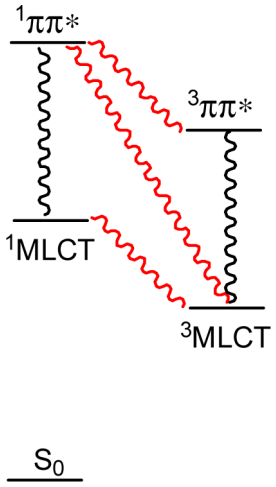

Figure 11. A scheme of electronic states that may be involved in excited state/excited state configurational mixing. The black lines represent the mixing within a single spin manifold, and the red lines represent the mixing via spin−orbit coupling between different spin manifolds.

The singlet states that seem most likely to contribute are ^{1}MLCT[14,22,23,117] and $^1\pi\pi^*$ excited states, so the important major contributions to eq 11 are likely to be of the form $H_{^3CT,^1CT'}^{SOC} = \langle \Psi_{^3CT}^{dia} | H^{(SOC)} | \Psi_{^1CT'}^{dia} \rangle$, $H_{^3CT,^1\pi\pi^*}^{SOC} = \langle \Psi_{^3CT}^{dia} | H^{(SOC)} | \Psi_{^1\pi\pi^*}^{dia} \rangle$, and $\alpha_{^3CT,^3\pi\pi^*}^3 H_{^3\pi\pi^*,^1CT'}^{SOC}$; the $H_{^3\pi\pi^*,^1\pi\pi^*}^{SOC}$ contribution is not relevant to the ^{3}MLCT emission. Possible SOC contributions of ^{1}MLCT/$^1\pi\pi^*$ mixing are omitted since the resulting terms are of the form $\alpha_{^1CT',^1\pi\pi^*}^1 H_{^3CT,^1\pi\pi^*}^{SOC} < H_{^3\pi\pi^*,^1CT'}^{SOC}$. In order for the triplet and singlet spin states to interact, the frontier orbital symmetries must differ in such a way that the spin−orbit coupling matrix elements are nonzero. Since the ^{3}MLCT → S_0 relaxation is only allowed by SOC-promoted mixing with a higher energy state (or states) of singlet spin multiplicity, $\alpha_{CT,g} \approx 0$ for the direct $T_0 \rightarrow S_0$ transition. However, DFT modeling of the excited states of Ru-A complexes has also found that many of their $S_0 \rightarrow S_n$ transitions have very small oscillator strengths,[71,72] presumably due to small values of $H_{g,e}$ resulting from poor spatial orbital overlap, and the T_0 dπ−SOMO orbital composition of $[Ru(NH_3)_5pz]^{2+}$ correlates with HOMO−1 of S_0 (see Supporting Information Figures S8 and S9).[19] These observations indicate that there are constraints on the SOC-coupled ^{1}MLCT states in addition to spin symmetry. Equation 11 and the preceding comments lead to the following modification of eq 5 which treats the observed emissions as the sum of contributions of several SOC interactions:

$$\overrightarrow{M_{e,g}} \approx \sum_{CT'} \alpha_{^3CT,^1CT'}^{SOC} [1 + \alpha_{^1CT,^1\pi\pi^*} + \alpha_{^3CT,^3\pi\pi^*}] \overrightarrow{M_{^1CT',g}} + \sum_{\pi\pi^*} \alpha_{^3CT,^1\pi\pi^*}^{SOC} \overrightarrow{M_{^1\pi\pi^*,g}} + \ldots \quad (12)$$

This expression is much simpler if there becomes only one contributing ^{1}CT′ interaction and if $\alpha_{^1CT,^1\pi\pi^*}^1 \ll 1$:

$$\overrightarrow{M_{e,g}} \approx \alpha_{^3CT,^1CT'}^{SOC} [1 + \alpha_{^3CT,^3\pi\pi^*}] \overrightarrow{M_{^1CT',g}} + \alpha_{^3CT,^1\pi\pi^*}^{SOC} \overrightarrow{M_{^1\pi\pi^*,g}} + \ldots \quad (13)$$

Assuming that the radiative relaxation of triplet states to the ground state can occur only by means of a SOC mechanism

DOI: 10.1021/acs.inorgchem.6b00374
Inorg. Chem. 2016, 55, 7341−7355

and that the moments for CT → S_0 and $\pi\pi^*$ → S_0 transitions are orthogonal, then

$$(M_{e,g})^2 \approx (\alpha^{SOC}_{^3CT,^1CT'})^2[1 + 2\alpha_{^3CT,^3\pi\pi^*} + (\alpha_{^3CT,^3\pi\pi^*})^2]$$
$$(M_{^1CT',g})^2 + (\alpha^{SOC}_{^3CT,^1\pi\pi^*})^2(M_{^1\pi\pi^*,g})^2 + ... \quad (14)$$

In eq 14, we have assumed that $|M_{^3CT,g}| \approx 0$ and that the two transition moments from eq 13 are approximately orthogonal. Equation 14 and substitution as in eq 4 can be used to obtain the following expression for k_{RAD}

$$k_{RAD} \approx (h\nu_{ave})^3 C_r \eta^3 \{(\alpha^{SOC}_{^3CT,^1CT'})^2(\alpha_{^1CT',g})^2[1 + 2\alpha_{^3CT',^3\pi\pi^*}]$$
$$(\Delta\mu)^2_{^1CT',g} + (\alpha^{SOC}_{^3CT,^1\pi\pi^*})^2(\alpha_{^3CT,^1\pi\pi^*})^2(\Delta\mu)^2_{^1\pi\pi^*,g}$$
$$+ ...\} \quad (15)$$

where all parameters are considered to be averages over all emission components. The first term in eq 15 corresponds to the SOC-promoted mixing of triplet and singlet MLCT excited states, and the second and third terms correspond to the configurational and SOC-promoted mixings, respectively, of $\pi\pi^*$ character into the ^{3}MLCT excited state. The denominators of the $\alpha^{SOC}_{^3X,^1Y}$ mixing coefficients are of the form ($E^v_{^1Y}$ is the vertical energy from the PE minimum of state ^{3}X)

$$\Delta E_{^3X,^1Y} = E^v_{^1Y} - E_{^3X} = E_{^3X}\left(\frac{E^v_{^1Y}}{E_{^3X}} - 1\right) \approx h\nu_{ave}\left(\frac{E^v_{^1Y}}{h\nu_{ave}} - 1\right) \quad (16)$$

Provided that $E^v_{^3CT,^1X} \ll h\nu_{ave}$, the energy dependence observed for k_{RAD} is expected to be first order for a single chromophore. In this limit $k_{RAD}/h\nu_{ave}$ should be proportional to $(H^{SOC}_{^3CT,^1CT'})^2$ and nearly constant over the energy range where the inequality holds.

Our DFT modeling has found that there is considerable mixing of acceptor ligand π-bonding orbital character into the dπ−SOMO of Ru-bpy (see the corresponding orbital with the largest effective nuclear charge in Figure 14 of Lord et al.)[16] and of Ru-MDA (canonical dπ−α orbitals in Figure 6) chromophores. In the Ru-bpy chromophores, this mixing correlates with the energy dependent vibronic amplitudes as well as an "extra" energy dependence of k_{RAD}. The calculated mixing occurs within the triplet spin manifold, and the variations in vibronic sideband amplitudes with energy may imply variations in total emission intensity with energy. Related (excited state)/(excited state) mixing is expected to occur within the singlet spin manifold, and intensity stealing has been experimentally documented in the absorption spectra of the *trans*-[{$(NH_3)_5$RuNC}$_2$-Ru(py)$_4$]$^{4+,5+,6+}$ complexes (in this case, mixing of metal to metal CT states with ^{1}MLCT states).[118] Our observations on the emission spectra of Ru-A complexes can be interpreted with respect to the various terms in eq 14.

The denominator of $\alpha^{SOC}_{^3CT,^1CT'}$ depends mostly on the exchange integral and small orbital energy differences. The energies of MLCT excited states track the differences in ground state donor-ionization and acceptor-affinity energies (or the differences in electrochemical half-wave potentials),[16,71,119,120] and the energies of MLCT absorptions and emissions are strongly correlated (usually about 1:1).[18−21] Therefore, this mixing coefficient is not expected to vary much with energy over the range of observed values of $h\nu_{ave}$ consistent with the observations on the Ru-MDA complexes, provided that the remaining terms make smaller contributions. In contrast, one expects large variations in the denominator of $\alpha^{SOC}_{^3CT,^1\pi\pi^*}$, so that this, as well as $\alpha^{SOC}_{^3CT,^3\pi\pi^*}$ could contribute to the extra energy dependence of k_{RAD} found in the Ru-bpy chromophores.

The second term in eq 15 corresponds to mixings with the $^1\pi\pi^*$ excited state, and this contribution could account for both the extra energy dependence of k_{RAD} and the energy dependent relative vibronic amplitudes found in the emissions of Ru-bpy chromophores.

Since the energies of the $\pi\pi^*$ excited states are not strongly dependent on the effective nuclear charge of the Ru center, the denominators of the MLCT/$\pi\pi^*$ mixing coefficients increase as $h\nu_{ave}$ increases and these contributions should become insignificant when $\Delta E_{CT,\pi\pi^*}$ is sufficiently large so that k_{RAD} is only dependent on the SOC-promoted ^{3}MLCT/^{1}MLCT mixing. This appears to be the case for the Ru-MDA complexes, possibly due to a relatively high $\pi\pi^*$ energy and a relatively low ^{3}MLCT energy. The trend of values of k_{RAD} decreasing as $h\nu_{ave}$ is decreased which was observed for Ru-bpy chromophores and the observations on Ru-MDA chromophores in this report indicate that "pure" ^{3}MLCT emissions (SOC-promoted through ^{3}MLCT/^{1}MLCT mixing) are intrinsically weak in these systems.

CONCLUSIONS

The contrast of the observed energy dependencies of k_{RAD} on $h\nu_{ave}$ for the Ru-bpy and the Ru-MDA chromophores is striking. The observations reported here for Ru-MDA and those previously reported for Ru-bpy[24] chromophores suggest that the energy dependence of k_{RAD} and the intensities of "pure" MLCT emissions are intrinsically weak. Furthermore, one expects that the emission bandshapes for such an idealized "pure" MLCT transition, which in this context is a spin−orbit coupling promoted mixing with a ^{1}MLCT excited state, should also be approximately energy independent since the distortions of the ^{3}MLCT and the ^{1}MLCT excited states are probably very similar in magnitude. Both DFT and simple MO modeling show mixing between the Ru-centered dπ-SOMO and the aromatic acceptor ligand π-orbitals for high energy ^{3}MLCT excited states, indicating that the contrast in intensity stealing arises from the configurational mixing of ^{3}MLCT and $^m\pi\pi^*$(A) (m = 1 or 3) excited states with smaller values of the mixing coefficients, $(\alpha^{SOC}_{^3CT,^1\pi\pi^*})^2$ and/or $(\alpha^{SOC}_{^3CT,^1CT'})^2\alpha_{^3CT,^3\pi\pi^*}$, for the Ru-MDA chromophores. The intrinsic emission intensities are weak for "pure" MLCT excited states (i.e., not mixed with $\pi\pi^*$ excited states) for both the Ru-bpy and the Ru-MDA chromophores,[18,19] due at least in part to the much smaller oscillator strengths of the SOC-coupled ^{1}MLCT → S_0 transitions.

The 77 K nonradiative ^{3}MLCT decay rate constants of the Ru-MDA and Ru-bpy chromophores are surprisingly similar despite the reported differences in distortions of the aromatic acceptor ligands. This may be a consequence of the very large number of vibronic relaxation channels that arise from the large number of excited state distortion modes for these complexes.

ASSOCIATED CONTENT

Supporting Information

The Supporting Information is available free of charge on the ACS Publications website at DOI: 10.1021/acs.inorgchem.6b00374.

DOI: 10.1021/acs.inorgchem.6b00374
Inorg. Chem. 2016, 55, 7341−7355

Electrochemistry of complexes; 77 K emission spectra of *cis*-/*trans*-$[Ru(NH_3)_4(MDA)_2]^{2+}$; 77 K emission spectra; 77 K emission rate constants and quantum yield resonance−Raman and Huang−Rhys parameters; values of k_{NRD} calculated for various values of γ; XYZ coordinates of the calculated structures; ^{1}H NMR spectra; atom-numbering scheme of target complexes; alpha and beta components of SOMOs; dπ(Ru) and ligand-based π^* corresponding orbitals of dπ- and π^*-SOMOs; X-ray structure and calculated ground state bond lengths of target complexes; calculated interaction energies between the ^{3}MLCT Ru complexes and methanol; HOMOs and LUMOs of the ground S_0 states of Ru-bpy and Ru-MDA complexes; the highest energy MOs containing the lone pair of electrons on the nonbonded pz-N (PDF)

AUTHOR INFORMATION

Corresponding Authors

*E-mail: hbs@chem.wayne.edu.
*E-mail: 054971@mail.fju.edu.tw.
*E-mail: jfe@chem.wayne.edu.

Notes

The authors declare no competing financial interest.

ACKNOWLEDGMENTS

This work was funded in part (Y.J.C.) by the Ministry of Science and Technology (Taiwan, R.O.C.) through Grant NSC 101-2113-M-030-005, and in part (J.F.E. and H.B.S.) by the Division of Chemical Sciences, Geosciences, and Biosciences, Office of Basic Energy Sciences of the U.S. Department of Energy through Grant DE-FG02-09ER16120.

REFERENCES

(1) Gerfin, T.; Graetzel, M.; Walder, L. *Prog. Inorg. Chem.* **1997**, *44*, 345.
(2) Graetzel, M. *Inorg. Chem.* **2005**, *44*, 6841.
(3) Graetzel, M.; Moser, J.-E. In *Electron Transfer in Chemistry*; Balzani, V., Ed.; Wiley-VCH: Weinheim, Germany, 2001; Vol. *5*, p 589.
(4) Hagfeldt, A.; Graetzel, M. *Acc. Chem. Res.* **2000**, *33*, 269.
(5) Nazeeruddin, M. K.; Kay, A.; Rodicio, I.; Humphrybaker, R.; Muller, E.; Liska, P.; Vlachopoulos, N.; Graetzel, M. *J. Am. Chem. Soc.* **1993**, *115*, 6382.
(6) O'Regan, B.; Graetzel, M. *Nature* **1991**, *353*, 737.
(7) Jäger, M.; Freitag, L.; González, L. *Coord. Chem. Rev.* **2015**, *304*−*305*, 146.
(8) Barbara, P. F.; Meyer, T. J.; Ratner, M. *J. Phys. Chem.* **1996**, *100*, 13148.
(9) Ciesienski, K. L.; Hyman, L. M.; Yang, D. T.; Haas, K. L.; Dickens, M. G.; Holbrook, R. J.; Franz, K. J. *Eur. J. Inorg. Chem.* **2010**, *2010*, 2224.
(10) Ossipov, D.; Gohil, S.; Chattopadhyaya, J. *J. Am. Chem. Soc.* **2002**, *124*, 13416.
(11) Smith, N. A.; Sadler, P. J. *Philos. Trans. R. Soc., A* **2013**, *371*, 20120519.
(12) Boerner, L. J. K.; Zaleski, J. M. *Curr. Opin. Chem. Biol.* **2005**, *9*, 135.
(13) Farrer, N. J.; Salassa, L.; Sadler, P. J. *Dalton Transactions* **2009**, 10690.
(14) Yersin, H.; Rausch, A. F.; Czerwieniec, R.; Hofbeck, T.; Fischer, T. s. *Coord. Chem. Rev.* **2011**, *255*, 2622.
(15) O'Donnell, R. M.; Johansson, P. G.; Abrahamsson, M.; Meyer, G. J. *Inorg. Chem.* **2013**, *52*, 6839.
(16) Lord, R. L.; Allard, M. M.; Thomas, R. A.; Odongo, O. S.; Schlegel, H. B.; Chen, Y.-J.; Endicott, J. F. *Inorg. Chem.* **2013**, *52*, 1185.
(17) Mazumder, S.; Thomas, R. A.; Lord, R. L.; Schlegel, H. B.; Endicott, J. F. *Can. J. Chem.* **2014**, *92*, 996.
(18) Tsai, C. N.; Mazumder, S.; Shi, X.; Zhang, X. Z.; Schlegel, H. B.; Chen, Y. J.; Endicott, J. F. *Inorg. Chem.* **2015**, *54*, 8495.
(19) Tsai, C.-N.; Tian, Y.-H.; Shi, X.; Lord, R. L.; Luo, D.-W.; Schlegel, H. B.; Endicott, J. F.; Chen, Y.-J. *Inorg. Chem.* **2013**, *52*, 9774.
(20) Odongo, O. S.; Heeg, M. J.; Chen, Y.-J.; Xie, P.; Endicott, J. F. *Inorg. Chem.* **2008**, *47*, 7493.
(21) Xie, P.; Chen, Y.-J.; Uddin, M. J.; Endicott, J. F. *J. Phys. Chem. A* **2005**, *109*, 4671.
(22) Yersin, H.; Rausch, A. F.; Czerwieniec, R.; Hofbeck, T.; Fischer, T. *Coord. Chem. Rev.* **2011**, *255*, 2622.
(23) Day, P.; Sanders, N. *J. Chem. Soc. A* **1967**, 1536.
(24) Thomas, R. A.; Tsai, C. N.; Mazumder, S.; Lu, I. C.; Lord, R. L.; Schlegel, H. B.; Endicott, J. F.; Chen, Y. J. *J. Phys. Chem. B* **2015**, *119*, 7393.
(25) Gould, I. R.; Young, R. H.; Mueller, L.; Albrecht, C.; Farid, S. *J. Am. Chem. Soc.* **1994**, *116*, 8188.
(26) Ciofini, I.; Daul, C. A.; Adamo, C. *J. Phys. Chem. A* **2003**, *107*, 11182.
(27) Alary, F.; Heully, J.-L.; Bijeire, L.; Vicendo, P. *Inorg. Chem.* **2007**, *46*, 3154.
(28) Abrahamsson, M.; Lundqvist, M.; Wolpher, H.; Johansson, O.; Eriksson, L.; Bergquist, J.; Rasmussen, T.; Becker, H.-C.; Hammarström, L.; Norrby, P.-O.; Åkermark, B.; Persson, P. *Inorg. Chem.* **2008**, *47*, 3540.
(29) Alary, F.; Boggio-Pasqua, M.; Heully, J.-L.; Marsden, C. J.; Vicendo, P. *Inorg. Chem.* **2008**, *47*, 5259.
(30) Salassa, L.; Garino, C.; Salassa, G.; Gobetto, R.; Nervi, C. *J. Am. Chem. Soc.* **2008**, *130*, 9590.
(31) Borg, O. A.; Godinho, S. S. M. C.; Lundqvist, M. J.; Lunell, S.; Persson, P. *J. Phys. Chem. A* **2008**, *112*, 4470.
(32) Salassa, L.; Garino, C.; Salassa, G.; Nervi, C.; Gobetto, R.; Lamberti, C.; Gianolio, D.; Bizzarri, R.; Sadler, P. J. *Inorg. Chem.* **2009**, *48*, 1469.
(33) Jakubikova, E.; Chen, W.; Dattelbaum, D. M.; Rein, F. N.; Rocha, R. C.; Martin, R. L.; Batista, E. R. *Inorg. Chem.* **2009**, *48*, 10720.
(34) Heully, J.-L.; Alary, F.; Boggio-Pasqua, M. *J. Chem. Phys.* **2009**, *131*, 184308.
(35) Dixon, I. M.; Alary, F.; Heully, J.-L. *Dalton Transactions* **2010**, *39*, 10959.
(36) Jakubikova, E.; Martin, R. L.; Batista, E. R. *Inorg. Chem.* **2010**, *49*, 2975.
(37) Sun, Y.; El Ojaimi, M.; Hammitt, R.; Thummel, R. P.; Turro, C. *J. Phys. Chem. B* **2010**, *114*, 14664.
(38) Gottle, A. J.; Dixon, I. M.; Alary, F.; Heully, J.-L.; Boggio-Pasqua, M. *J. Am. Chem. Soc.* **2011**, *133*, 9172.
(39) Lebon, E.; Bastin, S.; Sutra, P.; Vendier, L.; Piau, R. E.; Dixon, I. M.; Boggio-Pasqua, M.; Alary, F.; Heully, J.-L.; Igau, A.; Juris, A. *Chem. Commun.* **2012**, *48*, 741.
(40) Österman, T.; Abrahamsson, M.; Becker, H.-C.; Hammarström, L.; Persson, P. *J. Phys. Chem. A* **2012**, *116*, 1041.
(41) Bloino, J.; Biczysko, M.; Santoro, F.; Barone, V. *J. Chem. Theory Comput.* **2010**, *6*, 1256.
(42) Scarborough, C. C.; Lancaster, K. M.; DeBeer, S.; Weyhermueller, T.; Sproules, S.; Wieghardt, K. *Inorg. Chem.* **2012**, *51*, 3718.
(43) Scarborough, C. C.; Wieghardt, K. *Inorg. Chem.* **2011**, *50*, 9773.
(44) Rotzinger, F. P. *Inorg. Chem.* **2014**, *53*, 9923.
(45) Tu, Y.-J.; Mazumder, S.; Endicott, J. F.; Turro, C.; Kodanko, J. J.; Schlegel, H. B. *Inorg. Chem.* **2015**, *54*, 8003.
(46) Adamo, C.; Le Bahers, T.; Savarese, d. M.; Wilbraham, L.; García, G.; Fukuda, R.; Ehara, M.; Rega, N.; Ciofini, I. *Coord. Chem. Rev.* **2015**, *304*−*305*, 166.
(47) Santoro, F.; Lami, A.; Improta, R.; Bloino, J.; Barone, V. *J. Chem. Phys.* **2008**, *128*, 224311.

DOI: 10.1021/acs.inorgchem.6b00374
Inorg. Chem. 2016, 55, 7341−7355

(48) Chen, Y.-J.; Xie, P.; Heeg, M. J.; Endicott, J. F. *Inorg. Chem.* **2006**, *45*, 6282.
(49) Odongo, O. S.; Heeg, M. J.; Chen, Y.-J.; Xie, P.; Endicott, J. F. *Inorg. Chem.* **2008**, *47*, 7493.
(50) Englman, R.; Jortner, J. *Mol. Phys.* **1970**, *18*, 145.
(51) Freed, K. F.; Jortner, J. *J. Chem. Phys.* **1970**, *52*, 6272.
(52) Birks, J. B. *Photophysics of Aromatic Molecules*; Wiley-Interscience: New York, 1970.
(53) Brunold, T. C.; Gudel, H. U. In *Inorganic Electronic Structure and Spectroscopy*; Solomon, E. I., Lever, A. B. P., Eds.; Wiley-Interscience: New York, 1999; Vol. *1*, p 259.
(54) Steinfeld, J. I. *Molecules and Radiation, an Introduction to Modern Molecular Spectroscopy*; MIT Press: Cambridge, MA, 1981.
(55) Strickler, S.; Berg, R. T. A. *J. Chem. Phys.* **1962**, *3*, 814.
(56) Gould, I. R.; Noukakis, D.; Gomez-Jahn, L.; Young, R. H.; Goodman, J. L.; Farid, S. *Chem. Phys.* **1993**, *176*, 439.
(57) Bixon, M.; Jortner, J.; Cortes, J.; Heitele, H.; Michel-Beyerle, M. E. *J. Phys. Chem.* **1994**, *98*, 7289.
(58) Mulliken, R. S.; Person, W. B. *Molecular Complexes*; Wiley-Interscience: New York, 1967.
(59) Newton, M. D. *Chem. Rev.* **1991**, *91*, 767.
(60) Newton, M. D. In *Electron Transfer In Chemistry*; Balzani, V., Ed.; Wiley-VCH: Weinheim, Germany, 2001; Vol. *1*, p 3.
(61) Cave, R. J.; Newton, M. D. *Chem. Phys. Lett.* **1996**, *249*, 15.
(62) Cave, R. J.; Newton, M. D. *J. Chem. Phys.* **1997**, *106*, 9213.
(63) Hush, N. S. *Prog. Inorg. Chem.* **1967**, *8*, 391.
(64) Miki, H.; Shimada, M.; Azumi, T.; Brozik, J. A.; Crosby, G. A. *J. Phys. Chem.* **1993**, *97*, 11175.
(65) Mukherjee, T.; Ito, N.; Gould, I. R. *J. Phys. Chem. A* **2011**, *115*, 1837.
(66) Bixon, M.; Jortner, J.; Verhoeven, J. W. *J. Am. Chem. Soc.* **1994**, *116*, 7349.
(67) Powell, B. J. *Coord. Chem. Rev.* **2015**, *295*, 46.
(68) Flurry, R. L., Jr. *Symmetry Groups*; Prentice-Hall, Inc.: Englewood Cliffs, NJ, 1980.
(69) Shin, Y. K.; Brunschwig, B. S.; Creutz, C.; Sutin, N. *J. Phys. Chem.* **1996**, *100*, 8157.
(70) Coe, B. J.; Harris, J. A.; Brunschwig, B. S.; Asselberghs, I.; Clays, K.; Garin, J.; Orduna, J. *J. Am. Chem. Soc.* **2005**, *127*, 13399.
(71) Allard, M. M.; Odongo, O. S.; Lee, M. M.; Chen, Y.-J.; Endicott, J. F.; Schlegel, H. B. *Inorg. Chem.* **2010**, *49*, 6840.
(72) Tsai, C.-N.; Allard, M. M.; Lord, R. L.; Luo, D.-W.; Chen, Y.-J.; Schlegel, H. B.; Endicott, J. F. *Inorg. Chem.* **2011**, *50*, 11965.
(73) Caspar, J. V.; Meyer, T. J. *Inorg. Chem.* **1983**, *22*, 2446.
(74) Kober, E. M.; Caspar, J. V.; Lumpkin, R. S.; Meyer, T. J. *J. Phys. Chem.* **1986**, *90*, 3722.
(75) Litke, S. V.; Ershov, A. Y.; Meyer, T. J. *J. Phys. Chem. A* **2014**, *118*, 6216.
(76) Anderson, B. L.; Maher, A. G.; Nava, M.; Lopez, N.; Cummins, C. C.; Nocera, D. G. *J. Phys. Chem. B* **2015**, *119*, 7422.
(77) Chang, J. P.; Fung, E. Y.; Curtis, J. C. *Inorg. Chem.* **1986**, *25*, 4233.
(78) Krentzien, H. J. Ph.D. dissertation, Stanford University, Stanford, CA, 1976.
(79) Ford, P.; Rudd, D. F. P.; Gaunder, R.; Taube, H. *J. Am. Chem. Soc.* **1968**, *90*, 1187.
(80) Creutz, C.; Taube, H. *J. Am. Chem. Soc.* **1969**, *91*, 3988.
(81) Gaunder, R. G.; Taube, H. *Inorg. Chem.* **1970**, *9*, 2627.
(82) Malouf, G.; Ford, P. C. *J. Am. Chem. Soc.* **1977**, *99*, 7213.
(83) Pavanin, L. A.; Novais da Rocha, Z.; Giesbrecht, E.; Tfouni, E. *Inorg. Chem.* **1991**, *30*, 2185.
(84) Plummer, E. A.; Zink, J. I. *Inorg. Chem.* **2006**, *45*, 6556.
(85) Tfouni, E.; Ford, P. C. *Inorg. Chem.* **1980**, *19*, 72.
(86) Zwickel, A. M.; Creutz, C. *Inorg. Chem.* **1971**, *10*, 2395.
(87) Curtis, J. C.; Sullivan, B. P.; Meyer, T. J. *Inorg. Chem.* **1983**, *22*, 224.
(88) Evans, I. P.; Spencer, A.; Wilkinson, G. *J. Chem. Soc., Dalton Trans.* **1973**, 204.
(89) Bryant, G. M.; Fergusson, J. E.; Powell, H. K. *Aust. J. Chem.* **1971**, *24*, 257.
(90) Demas, J. N.; Crosby, G. A. *J. Am. Chem. Soc.* **1970**, *92*, 7262.
(91) Demas, J. N.; Crosby, G. A. *J. Am. Chem. Soc.* **1971**, *93*, 2841.
(92) Lacky, D. E.; Pankuch, B. J.; Crosby, G. A. *J. Phys. Chem.* **1980**, *84*, 2068.
(93) Frisch, M. J.; Trucks, G. W.; Schlegel, H. B.; Scuseria, G. E.; Robb, M. A.; Cheeseman, J. R.; Scalmani, G.; Barone, V.; Mennucci, B.; Petersson, G. A.; Nakatsuji, H.; Caricato, M.; Li, X.; Hratchian, H. P.; Izmaylov, A. F.; Bloino, J.; Zheng, G.; Sonnenberg, J. L.; Hada, M.; Ehara, M.; Toyota, K.; Fukuda, R.; Hasegawa, J.; Ishida, M.; Nakajima, T.; Honda, Y.; Kitao, O.; Nakai, H.; Vreven, T.; Montgomery, J. A.; Peralta, J. E.; Ogliaro, F.; Bearpark, M.; Heyd, J. J.; Brothers, E.; Kudin, K. N.; Staroverov, V. N.; Kobayashi, R.; Normand, J.; Raghavachari, K.; Rendell, A.; Burant, J. C.; Iyengar, S. S.; Tomasi, J.; Cossi, M.; Rega, N.; Millam, J. M.; Klene, M.; Knox, J. E.; Cross, J. B.; Bakken, V.; Adamo, C.; Jaramillo, J.; Gomperts, R.; Stratmann, R. E.; Yazyev, O.; Austin, A. J.; Cammi, R.; Pomelli, C.; Ochterski, J. W.; Salvador, P.; Dannenberg, J. J.; Dapprich, S.; Parandekar, P. V.; Mayhall, N. J.; Daniels, A. D.; Farkas, O.; Foresman, J. B.; Ortiz, J. V.; Cioslowski, J.; Fox, D. J. *Gaussian Development Version*, Revision H.20; Gaussian, Inc.: Wallingford, CT, 2010.
(94) Becke, A. D. *J. Chem. Phys.* **1993**, *98*, 5648.
(95) Perdew, J. P. *Phys. Rev. B: Condens. Matter Mater. Phys.* **1986**, *33*, 8822.
(96) Perdew, J. P.; Burke, K.; Wang, Y. *Phys. Rev. B: Condens. Matter Mater. Phys.* **1996**, *54*, 16533.
(97) Andrae, D.; Haussermann, U.; Dolg, M.; Stoll, H.; Preuss, H. *Theoret. Chimica Acta* **1990**, *77*, 123.
(98) Francl, M. M.; Pietro, W. J.; Hehre, W. J.; Binkley, J. S.; Gordon, M. S.; DeFrees, D. J.; Pople, J. A. *J. Chem. Phys.* **1982**, *77*, 3654.
(99) Hariharan, P. C.; Pople, J. A. *Theoret. Chimica Acta* **1973**, *28*, 213.
(100) Marenich, A. V.; Cramer, C. J.; Truhlar, D. G. *J. Phys. Chem. B* **2009**, *113*, 6378.
(101) Seeger, R.; Pople, J. A. *J. Chem. Phys.* **1977**, *66*, 3045.
(102) Schlegel, H. B.; McDouall, J. J. In *Computational Advances in Organic Chemistry*; Ögretir, C., Csizmadia, I. G., Eds.; Kluwer Academic: Amsterdam, The Netherlands, 1991.
(103) Bauernschmitt, R.; Ahlrichs, R. *J. Chem. Phys.* **1996**, *104*, 9047.
(104) Pennington, R.; Keith, T.; Millam, J. M. Semichem, Inc.: Shawnee Mission, KS, 2009.
(105) Demas, J. N.; Taylor, D. G. *Inorg. Chem.* **1979**, *18*, 3177.
(106) Zambrana, J. J. L.; Ferloni, E. X.; Gafney, H. D. *J. Phys. Chem. A* **2009**, *113*, 13457.
(107) Harned, H. S.; Owen, B. B. *The Physical Chemistry of Electrolytic Solutions*, 3rd ed.; Reinhold Pub. Corp.: New York, 1958.
(108) Neese, F. *J. Phys. Chem. Solids* **2004**, *65*, 781.
(109) Hupp, J. T.; Williams, R. T. *Acc. Chem. Res.* **2001**, *34*, 808.
(110) McCusker, J. K. *Acc. Chem. Res.* **2003**, *36*, 876.
(111) Sun, Q.; Mosquera-Vazquez, S.; Lawson Daku, L. M.; Guénée, L.; Goodwin, H. A.; Vauthey, E.; Hauser, A. *J. Am. Chem. Soc.* **2013**, *135*, 13660.
(112) Sun, Q.; Mosquera-Vazquez, S.; Suffren, Y.; Hankache, J.; Amstutz, N.; Lawson Daku, L. M.; Vauthey, E.; Hauser, A. *Coord. Chem. Rev.* **2015**, *282*−*283*, 87.
(113) Fabian, R. H.; Klassen, D. M.; Sonntag, R. W. *Inorg. Chem.* **1980**, *19*, 1977.
(114) Kasha, M. *Discuss. Faraday Soc.* **1950**, *9*, 14.
(115) Maruszewski, K.; Bajdor, K.; Strommen, D. P.; Kincaid, J. R. *J. Phys. Chem.* **1995**, *99*, 6286.
(116) Thompson, D. G.; Schoonover, J. R.; Timpson, C. J.; Meyer, T. J. *J. Phys. Chem. A* **2003**, *107*, 10250.
(117) Flint, C. D. *J. Chem. Soc., Faraday Trans. 2* **1976**, *72*, 721.
(118) Macatangay, A. V.; Endicott, J. F. *Inorg. Chem.* **2000**, *39*, 437.
(119) Gorelsky, S. I.; Kotov, V. Y.; Lever, A. B. P. *Inorg. Chem.* **1998**, *37*, 4584.

DOI: 10.1021/acs.inorgchem.6b00374
Inorg. Chem. 2016, 55, 7341−7355

(120) Lever, A. B. P.; Dodsworth, E. S. In *Electronic Structure and Spectroscopy of Inorganic Compounds, Vol. II*; Lever, A. B. P., Solomon, E. I., Eds.; Wiley: New York, 1999; p 227.

DOI: 10.1021/acs.inorgchem.6b00374
Inorg. Chem. 2016, 55, 7341−7355